Penetration and Performance Testing of the HP³ Mole for the InSight Mars Mission

T. Wippermann[a], T.L. Hudson[b], T. Spohn[c], L. Witte[a], M. Scharringhausen[a], G. Tsakyridis[a,1], M. Fittock[a,1], O. Krömer[a,2], S. Hense[a], M. Grott[c], J. Knollenberg[c], R. Lichtenheldt[d]

[a] *DLR German Aerospace Center – Institute of Space Systems,*
Robert-Hooke-Str. 7, 28359 Bremen, Germany,
Email: torben.wippermann@dlr.de

[b] *Jet Propulsion Laboratory, California Institute of Technology*
4800 Oak Grove Dr, Pasadena, CA 91109, USA

[c] *DLR German Aerospace Center – Institute of Planetary Research,*
Rutherfordstr. 2, 12489 Berlin, Germany

[d] *DLR German Aerospace Center – Institute of System Dynamics and Control,*
Münchener Str. 20, 82234 Weßling, Germany

[1] *now at OHB, Bremen, Germany*

[2] *now at Airbus - Airborne Solutions, Bremen, Germany*

Abstract

During the development and the qualification of the Heat Flow Physical Properties Package (HP³) instrument (developed by the German Aerospace Center), which is part of the NASA Mars mission InSight, its self-propelling subsurface probe, the HP³ Mole was used in several penetration tests. Here, the performance of the Mole to reach the target depth, to avoid or overcome obstacles on its path, and its directional stability in the subsurface is elaborated. The different test beds and set ups are described and the results are presented. The deep penetration tests (DPT), with the purpose to reach the target depth, are the most important performance tests and therefore the results are investigated in more detail in section 2. Full functional tests (FFT), which showed the performance and degradation of the mechanism inside the Mole, are presented in section 3. Additional penetration and life cycle tests are described in section 4. The testing has demonstrated that the HP³ Mole meets all of its penetration requirements with margin.

Keywords: InSight; HP³ Mole; heat flow; Mars exploration; penetrator; probe-soil-interaction

1. Introduction

InSight, Interior Exploration using Seismic Investigations, Geodesy and Heat Transport, is a Mars mission led by NASA's Jet propulsion Laboratory (JPL), which was launched on May 5th 2018 and landed on November 26th 2018. The purpose of this mission is to perform seismology on Mars by the SEIS instrument (developed by Centre National d'Études Spatiales (CNES)), rotational dynamics by the RISE instrument (developed by JPL) and to measure Mars' interior heat flux by the HP³ instrument (developed by Deutsches Zentrum für Luft- und Raumfahrt (DLR)) (Banerdt et al., 2013). An overview of the InSight lander and its instruments is shown in Figure 1.

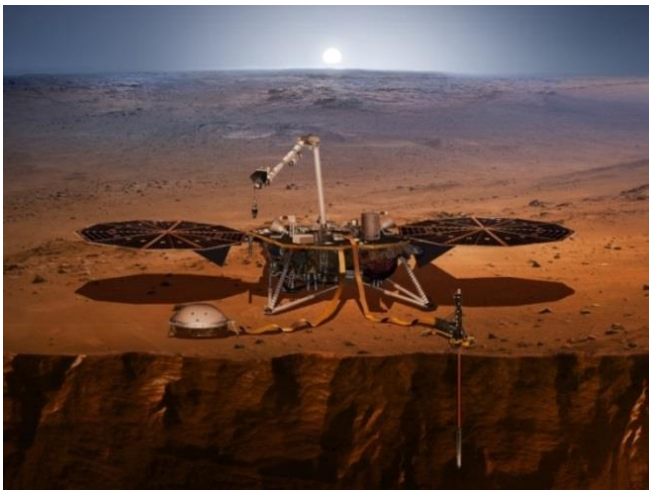

Figure 1: InSight lander with deployed instruments SEIS (beneath its wind and thermal shield at bottom left) and HP³ (bottom right) with Mole partially penetrated into the subsurface, and instrument RISE on the lander deck (antennas next to solar panels) (NASA/JPL-Caltech, 2018)

1.1. Heat flow and Physical Properties Package – HP³

The Heat Flow and Physical Properties Package HP^3 has been described in a recent publication by Spohn et al. (2018). Therefore, this section is restricted to a brief description of the package before the testing of the Mole is described in detail. To measure heat flux from Mars' interior at the InSight landing site, two quantities must be obtained: the thermal conductivity of the regolith and the thermal gradient. The thermal gradient must be measured at depths where surface temperature perturbations are smaller than the geothermal heat flux. HP^3 uses the Mole and its attached Science Tether to achieve this goal by measuring the temperature with an array of sensors distributed over the depth the Mole will reach.

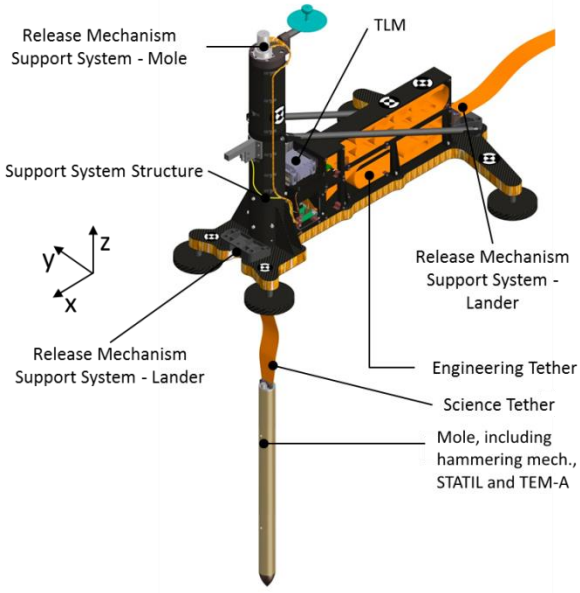

Figure 2: The HP³ instrument with its subsystems (Reershemius et al., 2018), not shown are BEE and RAD

Figure 2 is an overview of the HP³ subsystems. The Mole is a self-propelled penetrator connected to the Science Tether, which is a 5 m long flat-wire ribbon cable instrumented with temperature sensors. The goal of the Mole is to penetrate into the subsurface at the InSight landing site to a depth of at least 3 m (up to maximum of 5 m) and pull the instrumented Science Tether with it. The hull of the Mole contains heater foils, called the Thermal Excitation Measurement - Active (TEM-A), that are used to conduct thermal conductivity measurements periodically, every 0.5 m of achieved depth, as the Mole penetrates. The Science Tether is embedded with 14 high-precision temperature sensors, called the Thermal Excitation Measurement - Passive (TEM-P). Once emplaced, this (approximately) vertical array of temperature sensors measures the subsurface thermal gradient.

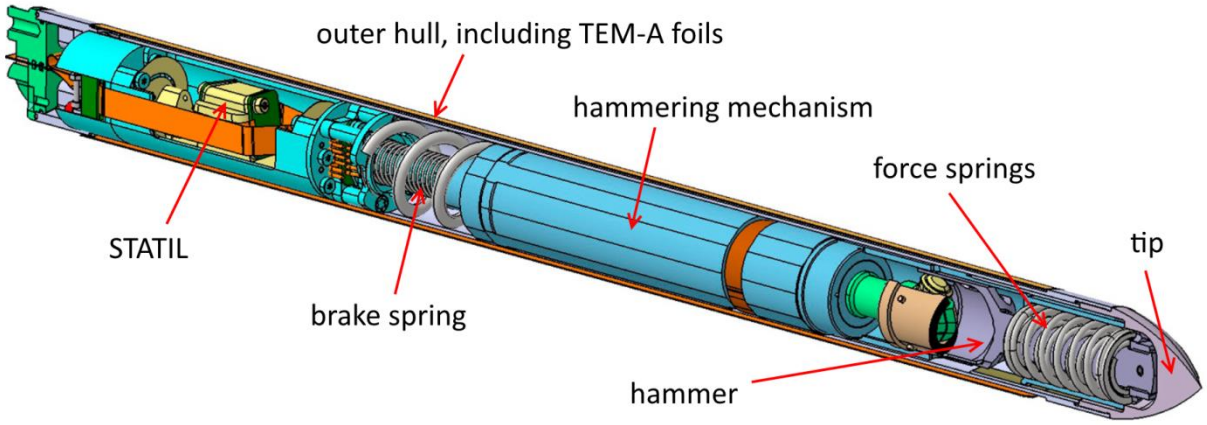

Figure 3: Major components of the Mole (CAD model) – hammering mechanism, including hammer, force springs and brake spring (right), STATIL (left) and outer hull, including TEM-A foils and tip (cut to display internal components) (Spohn et al., 2018)

In Figure 3 the Mole is shown with its internal components. The mechanism to realize the penetration is a hammer-and-anvil-like system, where the hammer is repeatedly compressed against a set of springs. These force springs are continuously loaded until a sudden release, which causes the hammer to accelerate towards and strike the inside of the Mole's tip (the anvil). This cycle is repeated successively and with each cycle the Mole is pushed further into the soil by a few millimeters to a fraction of a millimeter (depending on the depth of the Mole). The displacement of the Mole is reached by pushing the soil aside with the tip of the Mole while compacting the soil in the near vicinity of the tip. This increases the local relative density of the soil. In the same time the static friction of the side walls of the Mole to the soil is overcome by the impact caused by the hammer strokes. The rebound of the hammering mechanisms is dampened by a soft spring, called brake spring, resulting in upward-directed rebound of the Mole that cannot overcome the static friction of the soil on the hull. Therefore a friction force between Mole sidewalls and soil is essential for the Mole progression.

It is essential to HP^3 science that the final depths of the TEM-P sensors in the Science Tether are known to an uncertainty of <2 cm. The subsurface path of the Mole may deviate from perfectly vertical due to irregularities in soil density or subsurface rocks. Two ancillary sensors allow reconstruction of the subsurface path of the Mole, thereby determining the final depth of the TEM-P sensors. These ancillary sensors are a STAtic TILtmeter (STATIL) within the body of the Mole, which reports its orientation with respect to the local gravity vector. Within the Support System is the Tether Length Monitor (TLM), an optical system that reads relative and absolute depth markings on the sides of the Science Tether, thereby reporting the amount of tether extracted by Mole penetration. Combining these measurements allows the path of the Mole and the depth of the TEM-P sensors to be calculated. The Support System accommodates all of the aforementioned subsystems, launch locks, further sensors and the Engineering Tether, which provides the power and data interface of the HP³ instrument to the lander deck. Within the lander is the Back-End Electronics (BEE), which controls all HP^3 functions including data pre-processing and packaging for transfer to the lander for return to Earth. A further component of HP^3 is a radiometer (RAD) installed below the lander deck to observe surface brightness temperatures as inputs to subsurface thermal modelling.

Due to delays on crucial hardware, the first planned launch for InSight in March 2016 could not take place. As the decision was made to postpone the launch to 2018, DLR took the chance to improve the design of the Mole. This resulted in two different HP³ flight models with respective qualification models. They were built and tested in 2015, respectively 2017.

The HP³ Mole is the second application of the concept of self-propelling moles in a space mission. The first usage was the Planetary Underground Tool (PLUTO) on the Beagle 2 lander of ESA's 2003/2004 Mars Express mission.

1.2. Mole system requirements

The science mission requirements regarding the HP³ experiment are described by Spohn et al. (2018). In order to fulfil them, the Mole has to comply with a set of its own set of requirements. The most relevant requirements for the performance testing are listed in Table 1. As described in the following sections of this paper, they were achieved with margin.

ID	requirement
L5-TM-1	The Mole shall penetrate to a depth of at least 3 m into representative Mars simulants (MMS < 2 mm and WF-34)
L5-TM-3	The Mole shall be capable of executing no fewer than 20 000 strokes in a regolith with properties as in L5-TM-1
L5-TM-4	The Mole shall be capable of reaching 3 m depth under earth ambient conditions into representative Mars simulants (MMS < 2 mm and WF-34) within 24 hours of cumulative hammering

Table 1: List of Mole system requirements relevant for performance testing

Additionally, several requirements state that all dynamically stressed components shall still be operational with a specified performance after fulfilling the lifetime requirement (L5-TM-3).

1.3. Mole models

During the course of the InSight project, several different models were designed and tested. Further details on the design of the Mole are described by Spohn et al. (2018). The early models include one Mechanical Mole Model (referred to as MMM), one Breadboard Models (BBM) and three early Prototype models (PT). The hammering mechanisms (HM) for the MMM, BBMs, and PTs were designed by DLR's Institute of Space Systems and built on inherited hammering mechanism designs from before the InSight project was officially selected by NASA. Due to problems with the performance and reliability of the hammering mechanism, its design was completely reworked. The new hammering mechanisms were designed by the Centrum Badań Kosmicznych (CBK) and Astronika, both located in Warsaw, Poland. The new Mole models were divided into two groups: Protoflight Models (referred to as PFM) were used as flight (PFM-1) and flight spare (PFM-2) models, while Protoflight Equivalent Models (PFEs 1-3), which are of the same design, were designated for performance and qualification tests. Before the first PFE model was designed, a preliminary version of the hammering mechanism was built to show its new capabilities. This model is referred to as preliminary protoflight model (PPFM) and the Mole it was installed into changed over time. At first this Mole model was a simple housing with two cables connected to the motor of the hammering mechanism. Later this model was further upgraded to become a good comparison to the actual PFE and PFM models with the exception of the stroke cycle duration. Due to a different motor installed in the PPFM model, its stroke cycle duration is less than half of the other models.

Mechanism life testing in 2015 and 2016 revealed design flaws that adversely affected Mole robustness. When the InSight launch was delayed from March 2016 to May 2018, the time provided by the delay was used to design and build two new Mole models that addressed these deficiencies. Those models were called the QM Mole (used for qualification testing) and the PFM-3 Mole, which became the new flight unit. The design of the hammering mechanism remained unchanged and so does the general penetration performance of the Mole models.

Model name	Preliminary Protoflight Model (PPFM)	Protoflight Equivalent Model 1 (PFE-1)	Protoflight Equivalent Model 2 (PFE-2)	Protoflight Equivalent Model 3 (PFE-3)	Protoflight Model 1 (PFM-1)	Protoflight Model 2 (PFM-2)	Qualifica-tion Model (QM)	Protoflight Model 3 (PFM-3)
Purpose	Demonstrator for new hammering mechanism (HM) design	Penetra-tion test model	Subsystem test model	Life test unit for PFM-1 & PFM-2	Flight model (relegated to Flight spare after PFM-3 built)	Flight spare (unused after PFM-3 built)	Life test unit for PFM-3	Flight model
1st creation date	Feb. 2014	Aug. 2014	Jan. 2015	Jul. 2015	Apr. 2015	Oct. 2015	Mar. 2017	Jun. 2017
Outer dimensions - Mole	Ø 27 mm x 300 mm (DPT1 - DPT3); 400 mm (after DPT3)	Ø 27 mm x 400 mm	Ø 27 mm x 400 mm	Ø 27 mm x 400 mm	Ø 27 mm x 400 mm	Ø 27 mm x 400 mm	Ø 27 mm x 400 mm	Ø 27 mm x 400 mm
Outer dimensions - Science Tether	Ø 4 mm steel rope & cables (DPT1); 36 mm wide flat ribbon cable (after DPT1)	36 mm wide flat ribbon cable	36 mm wide flat ribbon cable	36 mm wide flat ribbon cable	36 mm wide flat ribbon cable	36 mm wide flat ribbon cable	36 mm wide flat ribbon cable	36 mm wide flat ribbon cable
Mass	0.90 kg	0.90 kg	0.93 kg	0.93 kg	0.93 kg	0.93 kg	0.93 kg	0.93 kg
Stroke cycle duration	1.7 - 1.9 s	3.6 - 3.9 s	3.6 - 3.9 s	3.6 - 3.9 s	3.6 - 3.9 s	3.6 - 3.9 s	3.6 - 3.9 s	3.6 - 3.9 s
Stroke frequency	0.53 - 0.59 Hz	0.26 - 0.28 Hz	0.26 - 0.28 Hz	0.26 - 0.28 Hz	0.26 - 0.28 Hz	0.26 - 0.28 Hz	0.26 - 0.28 Hz	0.26 - 0.28 Hz
Nominal force spring energy	0.84 J (DPT1 – DPT4); 0.70 J (after DPT4)	0.85 J	0.70 J	0.70 J	0.70 J	0.70 J	0.70 J	0.70 J
Nominal stroke force (measurement see 3.1)	1150 N	n/a	1020 N	1070 N	1240 N	1180 N	1140 N	1180 N

Table 2: Mole model overview listing all models with the flight model hammering mechanism design. The design of the hammering mechanisms for the MMM, BBM and PT models is significantly different from these models and are therefore not listed

The tests shown in this paper mostly focus on tests of the PPFM, PFE, QM, and PFM models. In Table 2 all Moles since the PPFM model are compared by their penetration-relevant properties. Further tests were conducted for the other subsystems of the instrument. The results and design description of the Support System were compiled by Reershemius et al. (2018).

1.4. Regolith used for penetration tests

The purpose of the penetration tests was in part the development and the qualification of the Mole. Penetration results also informed the landing site selection process and helped in the risk assessment with the chosen landing site. The subsurface at the landing site was and will be the biggest unknown for the InSight mission until the HP³ Mole begins to penetrate. Since no other previous Mars mission recorded any data about the composition of the soil beneath a couple of centimeters, the biggest part of the soil the Mole has to penetrate through can only be estimated from what can be seen on the surface (Golombek et al., 2017). To bracket subsurface properties (e.g., particle size, particle shape, size distribution, relative density, presence of rocks) that may affect the penetration success of the HP^3 Mole, various test media and obstacles were used for the different penetration tests. The three simulants used for most of the penetration tests are WF 34, a nearly cohesion-less quartz sand of the German company Quarzwerke GmbH, Lake Herman Basalt or "Syar" (after the company it was provided from), a high cohesion mixture of mechanically crushed basaltic sand and dust from northern California and MMS <2mm, a mechanically crushed Saddleback Basalt from the Mojave desert in California. These soils were originally selected as they represent a wide spectrum of properties, e.g. in terms of cohesion. Below these soils are compared visually (Figure 4 and Figure 5), in their geophysical properties (Table 3) and their particle size distribution (Figure 6). In Table 3 the MMS Dust mentioned in section 4.4 is listed as well, but outside of this test, this soil was not used for any activities mentioned in this paper.

Figure 4: Macroscopic pictures of WF 34 (left), Syar (middle) and MMS <2mm (right)

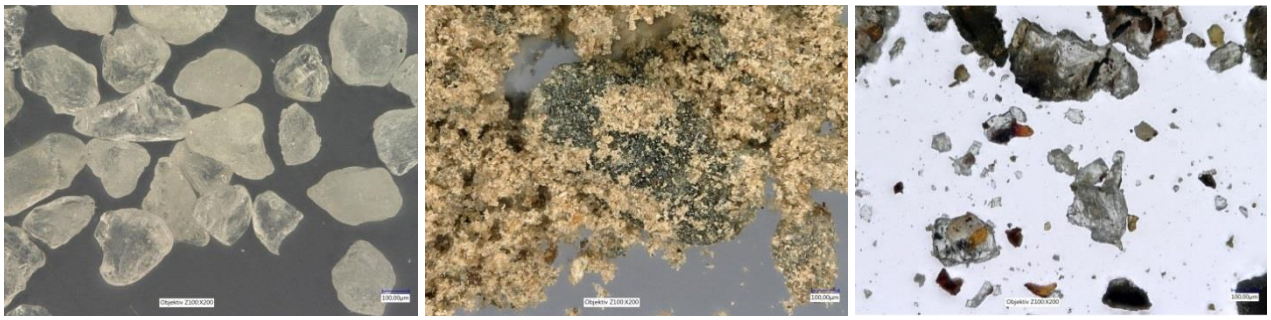

Figure 5: Microscopic pictures of WF 34 (left), Syar (middle) and MMS <2mm (right) with magnification of 200x

Regolith	WF 34	Syar	MMS <2mm	MMS Dust
Median grain size (D50)*	0.213 mm	0.946 mm	0.283 mm	0.024 mm
Effective grain size (D10)*	0.141 mm	0.011 mm	0.025 mm	0.003 mm
Uniformity coefficient	1.6	122	13.7	9.23
Cohesion, failure	0.00 kPa	4.02 kPa	3.53 kPa	1.96 kPa
Friction angle, failure	32°	54.8°	46.4°	38.1°

Table 3: Regolith properties for used simulants *: All particles equal or less than stated value contribute to 50 % resp. 10 % of the total weight

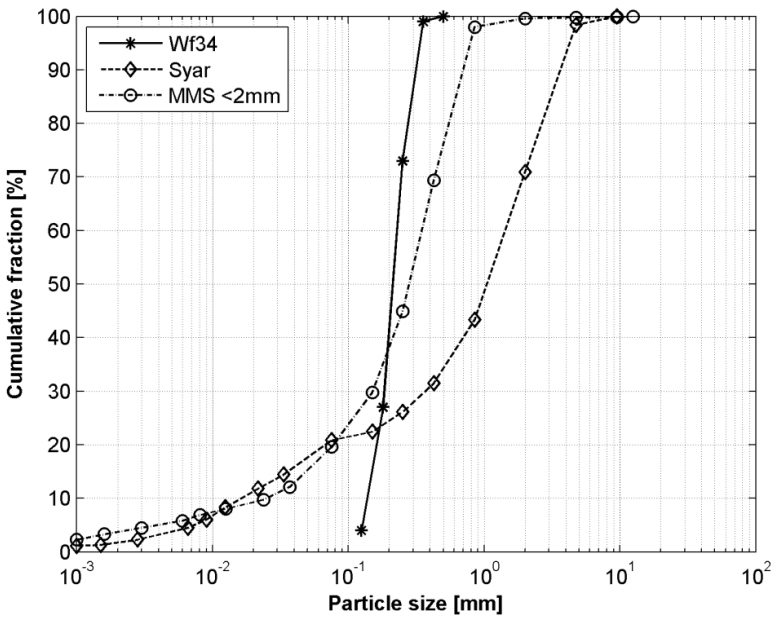

Figure 6: Particle size distribution for used simulants

1.5. Considerations on influence of gravity on testing

All of the described tests in soil with the Mole were conducted under Earth gravity as the amount of soil to pass the depth requirement of at least 3 m and the long duration of a single test run (in a range of several hours) do not permit low gravity flights. Other means of compensation were considered, but found not feasible to implement in the scale of this project. A tilted test in soil would reduce the influence of gravity along the direction of advance for the Mole, but would in turn increase the frictional forces on the side walls of the Mole. Additionally would the non-symmetric stress conditions at the tip due to soil weight and the self-righting of the Mole due to its center of mass near the tip impact the penetration performance of the Mole and comparability of the test results to Mars gravity. Another option would be to adapt the soil to match expected soil properties on Mars under Earth gravity by selecting appropriate macroscopic properties like friction angle, bulk density and cohesion. The influence of gravity on soil mechanics is mainly due to the frictional forces on grain-level, which would be different in this case compared to the properties expected on Mars.

To a degree the latter option was considered by the choice of using WF 34. Due to its narrow particle size distribution, that shows low compactability, the influence of gravity on the compaction was relatively low with this soil, but still higher than what is expected on Mars. Simulations gave a ratio between Mars and Earth penetration performance for the same microscopic soil parameters. The macroscopic parameters were changed with the different gravities. The calculated factor was ~1.33:1 Mars:Earth for the Mole's penetrated depth per stroke cycle (Lichtenheldt et al. 2016 p.151). Furthermore the Mole was simulated with simplified soil models for Martian gravity after every design change and several simulation scenarios on Earth and Mars were used to check acceptability of the different Mole models including the FM Mole. So with this approach the penetration testing on Earth were performed as a worst case scenario. If the Mole was able to overcome the soil resistance of comparable soil on Earth and was able to conduct the higher number of strokes required to do so, it is able to perform accordingly on Mars.

2. Deep Penetration Test

The primary and most realistic performance tests of the Mole are the deep penetration tests (DPT). In these tests, the Mole has to penetrate as far as possible into a regolith column. As listed in section 1.2 and described by Grott et al. (2010) the required depth for the Mole to reach, in order to allow the heat flow measurement with the desired accuracy, is 3 m. The maximal possible depth with the hardware and testbed is 5 m. During the course of the InSight project, a variety of configurations in the test setup and the Mole itself were tested. The used soils in this testbed were WF 34 and Syar (details in section 1.4).

All Mole models except the very early MMM were tested in the DPT facility and some design concepts were investigated. The extent to which the hardware was operated varied from hammering-only tests powered directly from power supplies to full runs through the operational sequence planned for Mars, using flight-like control and feedback electronics, as described in Spohn et al (2018).

The preparation of the DPT, the test, and the evaluation afterwards are very work intensive, requiring the following tasks:

- a fresh fill of the testbed no more than a few days before the actual penetration. This reduces the time for external forces (e.g., seismic or anthropogenic ground motions) to compact the column and changing the initial conditions
- characterization of the soil before the test
- setting up all test equipment
- performance of the deep penetration test
- build-down of the test equipment
- characterization of the soil after the test
- careful excavation of the Mole and Science Tether from the testbed
- several fill height measurements of the soil before and after the listed steps

The tasks and the technical equipment are described in more detail below.

2.1. Testbed and test preparation

The primary testbed for the deep penetration tests is located at DLR Bremen. It is a 5.5 m tall metal tube with a diameter of 0.8 m. This size was chosen so that the wall effect is reduced. This effect appears when the Mole gets too close to the side walls or the bottom of the testbed. As the Mole approaches a testbed boundary, the soil between the Mole and the boundary gets more compacted (due to the immovable wall) than it would in an unrestricted real space. More highly compacted soil impedes the penetration performance. A larger-diameter testbed more closely simulates unrestricted soil on Mars. The actual testbed diameter of 0.8 m is a compromise between larger diameters which would involve significantly more volume of simulant material and therefore more time and effort to prepare and the available

resources at hand during the project. The tube is built out of 5 segments of 1 m and one of 0.5 m in length to simplify the adaption of the testbed to other future missions. The test stand is shown in Figure 7.

On top of the tube is a platform which gives the test conductors some space to work. This platform is not put on the tube itself, but instead mounted on a scaffold. This decouples any shocks created by working on the platform from the soil, to again reduce uncontrolled sources of soil compaction. A ladder on the scaffold and the laboratory crane allow relatively easy access to the platform for personnel and equipment.

To fill and empty the testbed an industrial pneumatic vacuum conveyor specifically modified to move soil is used. This device is 'powered' by high pressure air generated by an external air compressor. An approx. 6 m long hose is connected to the vacuum conveyor, where the soil is sucked in. Individual 'lifts' of soil of a few liters are sucked into the conveyor body every few seconds. At the end of each cycle, the vacuum is automatically diverted and a valve on the lower body opens and drops the soil, which falls under gravity through ambient air, to the top of the growing soil column. This results in self-compaction and the final soil column has a rough increase in density from top to bottom (this depends on mechanical properties of the emplaced soil). To increase the repeatability of the DPTs, the vacuum conveyor was put in the same position for every test during filling. The soil was dropped into the testbed with the vacuum conveyor being at the same height as the top rim of the testbed and as close as possible to the center. This deviation from a procedure for high-precision soil mechanics test was a compromise necessary to be done with this testbed and the available facilities. As the soil characteristics were measured with a penetrometer for several fillings of the testbed (described in section 2.4), the knowledge of the soil condition during the tests was sufficient for this project.

Figure 7: Deep penetration testbed (left) with penetrometer (top) and vacuum conveyor (bottom right)

2.2. Test setup

The setup for the test equipment changed depending on the desired measurements and available completeness of the flight configuration. The complete set consists of the Mole, a miniature version of the Support System (Mini S/S) with an integrated Tether Length Monitor (TLM), and the Back End Electronics (BEE). The Mini S/S with Mole, Science Tether, and TLM rests on the top of the soil column. The proximal end of the Science Tether, emerging from the tether storage compartment in the Mini S/S, is connected to the BEE on the work platform. The BEE is connected to a power supply and a control laptop for sending commands and receiving the recorded data. In a complete test setup, all subsystems inside the Mole (motor current, motor temperature sensor, heaters, and STATIL) and the TLM are

recording. Those measurements are processed by the BEE and result in motor current, various temperatures inside the Mole, temperatures of the TEM-P sensors in the Science Tether, the STATIL axis orientations and the extracted tether length. The STATIL-reported Mole attitude and the tether length extracted are combined to compute the actual Mole tip depth. The setup is all done in an ESD-safe area to protect the sensitive electronics.

To observe the progress of Science Tether extraction from the Mini S/S and the progress of the Science Tether and Mole into the soil, a camera was installed on top of the testbed. The camera was set to time-lapse mode, saving a picture of the test setup once every 10 seconds. During early phases of the project, when either the TLM or STATIL were absent from the test, this video was used to reconstruct the performance of the Mole. Therefore the Science Tether was marked every 100 mm. An example for such a time-lapse video can be found in

Video 1 (https://mars.nasa.gov/resources/22080/time-lapse-of-the-hp3-mole, NASA, 2014).

Video 1: Time-lapse of the PPFM DPT4 test conducted at the DPT facility of the DLR Institute of Space Systems. Published on NASA (2014)

2.3. Test results

All acquired test data for time, Mole tip depth, and the calculated penetration rates are listed in Appendix A. The penetration rate was calculated with the central difference quotient of tip depth divided by time. It is displayed in all diagrams as function of depth rather than time, as the penetration rate-time plots do not properly show the highly dynamic behaviour of the first 3 m (approx. 60 to 180 minutes), but show more detail than necessary in the relatively steady section of below 3.5 m (approx. 120 to 720 minutes). The tip depth is always plotted along the vertical axis and in descending order for better comparison and visualization of the results.

As shown in Table 2, the stroke frequency of the PPFM Mole model is higher than of the other Mole models. For a better comparison of the PPFM test data, its stroke frequency was scaled to an average stroke frequency of the other tested Moles. As this virtually elongates the time between strokes for the PPFM model the time values were scaled by a factor of 2.19 and the penetration rate values in mm/min were scaled by a factor of 0.46 compared to the measured values in reality.

The Mole reached the required 3 m at Earth gravity in a number of cases and all within the maximum duration of 24 hours. For some of the earlier tests with the models PPFM and PFE-1, the DPTs had to be aborted due to technical reasons. After implementing dedicated design changes, that enhanced the durability and reliability of the Mole, later tests to reach 3 m did not fail. It should be mentioned, that some tests had to be aborted before reaching the maximal depth of 5 m due to limited time during the project. Some tests were conducted by the Jet Propulsion Laboratory in a 3 m test bed and with the use of the MMS <2mm soil as test medium. By reaching the terminal depth, the second mentioned soil depth requirement was fulfilled.

2.3.1. Test comparison for Quartz sand WF34

For the DPTs in WF34 a variety of tests were conducted. In Figure 8 all deep penetration tests in quartz sand with similar configurations and reaching a depth of at least 3 m are compared. The graphs for the PPFM DPT6 and the PFE-1 DPT2 were cut at 720 minutes in the depth-time curves for clarity. These tests reached 5 m after 1300 minutes (PPFM DPT6; with scaled time 2900 minutes) and 4.85 m after 1500 minutes (PFE-1 DPT2). The variance between the test results can be traced back mainly to the filling method described in 2.1. All depth vs. time profiles show a similar trend:

- A steep section from the start until 20 to 40 minutes in the test, reaching 1.0 to 1.6 m.
- A nearly linear phase from 1.0 – 1.6 m until 2.0 – 3.0 m (from now on referred to as intermediate phase), where the different test runs start to spread.
- A knee section from 2.0 – 3.0 m until 2.8 – 3.8 m.
- A second nearly linear phase below 2.8-3.8 m with low progression over time (from now on referred to as deep phase).

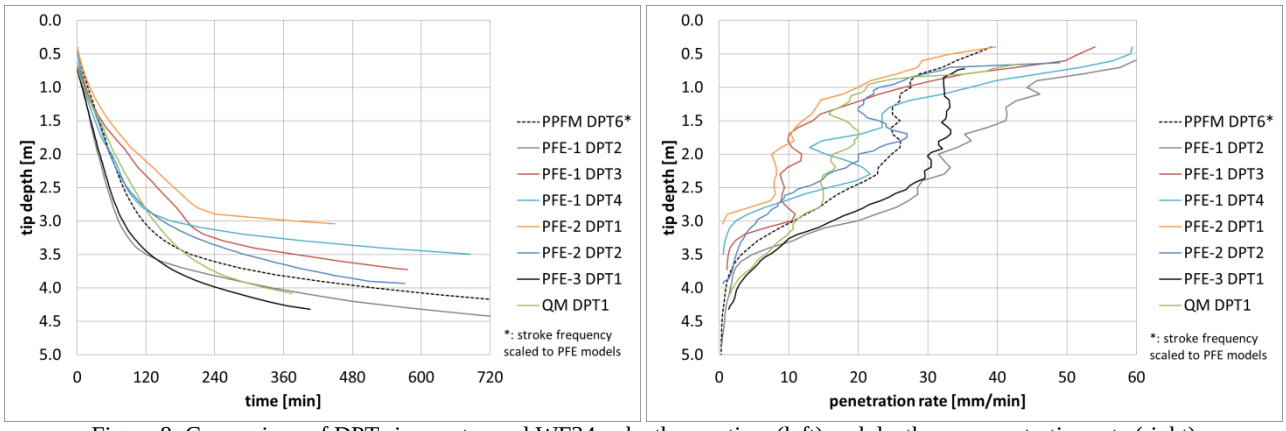

Figure 8: Comparison of DPTs in quartz sand WF34 – depth over time (left) and depth over penetration rate (right)

When comparing the curves of depth over penetration rate, the DPTs can be sorted by their intermediate phase into three groups:

1. Low penetration rates of 8-12 mm/min in the intermediate phase (red/orange in Figure 8):

In the first part (up till 1.6 m), these curves show a lower deceleration of the Mole over a longer distance, when compared to the other test runs. In this section the curves follow more a shape of a square root function rather than a linear progression. Afterwards the penetration rate stays relatively steady (within the margin of error) until 2.7 – 3.0 m. There it drops down to less than 2 mm/min within 0.3 m.

2. Moderate penetration rates of 10-30 mm/min in the intermediate phase (green/blue):

The first steep section lasts till 1.0 to 1.4 m and the penetration rate decreases rapidly, similar to the group of high penetration rates. The intermediate phase is vastly different than in the other groups. There the penetration rate oscillates within ± 2 to 5 mm/min around the mean average of this section. The depth increments between all vertices of these oscillations are approx. 0.4 m or one Mole length. The PFE-2 DPT2 and QM DPT1 were recorded with a BEE and a TLM, so the depth and time resolution is higher than on the other tests (with the exception of the PFE-3 DPT1 test, which was recorded with the same setup). Therefore the margin of error is a lot lower in these graphs and the oscillatory behaviour in the intermediate phase cannot be explained as a measurement artifact.

3. High penetration rates of more than 25 mm/min in the intermediate phase (grey/black):

The curves decrease rapidly and reach the intermediate phase at approximately 0.9 m. The penetration rates are then decreasing linearly, although with different slopes, until 2.5 m. From there the penetration rate drops within 0.8 – 1.0 m to the deep phase. The first part of the data of PFE-3 DPT1 with presumably higher penetration rates was not recorded properly and is therefore not displayed.

2.3.2. Test comparison for Syar

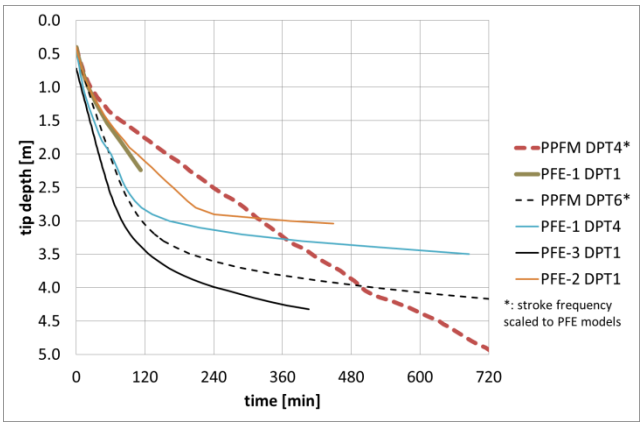

In

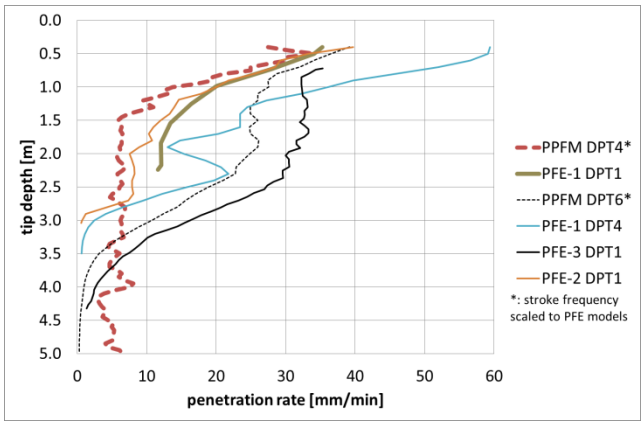

Figure **9** two DPTs with the PPFM and PFE-1 models in Syar are shown (thick lines). The PFE-1 DPT1 had to be aborted at a depth of 2.2 m due to an electrical problem. Both graphs show a similar progression than the DPTs in quartz sand for the start of the test. They start with a penetration rate of approx. 30 mm/min and decrease to values of 6 – 12 mm/min within the first 1.5 – 1.8 m. After 1.5 m the PPFM DPT4 then progresses with a nearly steady penetration rate of 4 – 6 mm/min with some fluctuation of up to 3 – 8 mm/min. Another significant drop in the penetration rate (e.g. like the knee in the quartz sand DPTs around 3 m) could not be observed during this test.

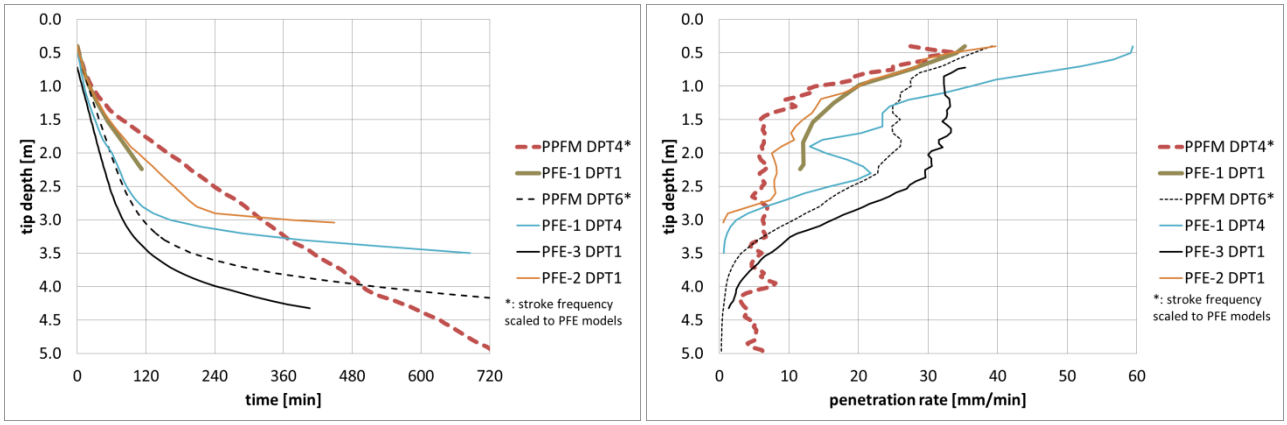

Figure 9: Comparison of PPFM DPTs in Syar (thick line) and quartz sand (thin line) - depth vs. time (left) and depth vs. penetration rate (right)

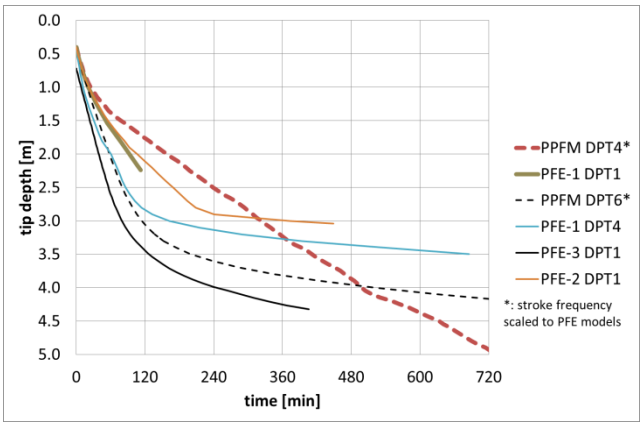

In

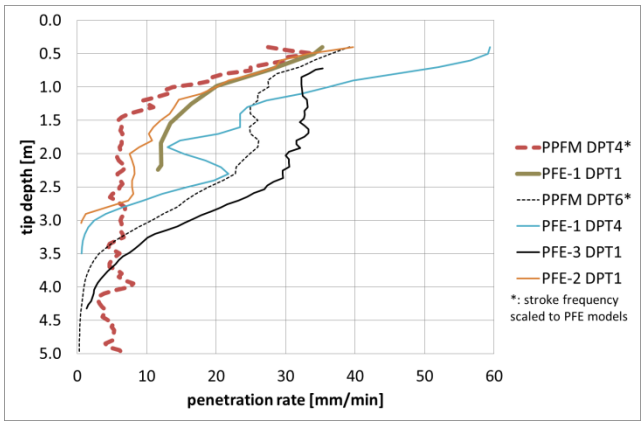

Figure **9** the DPTs in quartz sand and Syar are directly compared. The target depth of 3 m was reached in 70 – 190 minutes for quartz sand, resp. 375 minutes for PFE-2 DPT1 and in 320 minutes during the PPFM DPT4 in Syar. So only the worst DPT in quartz sand is comparable to the DPTs in Syar. Below 3 m the missing knee in the Syar DPT results in an overall better performance in Syar for reaching the maximum depth of 5 m.

The landing site selection progress, as described by Golombek et al. (2017), determined that a very low cohesive soil can be expected at the HP³ deployment site. Therefore, quartz sand WF 34 was considered a more accurate soil simulant than Syar. Additional considerations during the low pressure penetration testing (see section 4.2) led to the conclusion that Syar was disregarded as soil simulant.

2.3.3. Test comparison with and without installed tether

The very first version of the PPFM model consisted only of the hammering mechanism and a hull of similar shape as the later built Moles. A flat ribbon Science Tether to carry power to the Mole was not available. To supply power to the motor inside the hammering mechanism, two cables were routed through the Mole and tied to a steel rope at the back of the Mole. This provided strain relief to the cables as they were pulled by the Mole through the regolith simulant. With this configuration, the first test PPFM DPT1 was conducted in quartz sand. The sole purpose of this test was to show the capabilities of the new hammering mechanism design. As can be seen in Figure 10 the PPFM reached 4.9 m after 74 minutes (scaled to PFE stroke frequencies 162 minutes) in quartz sand.

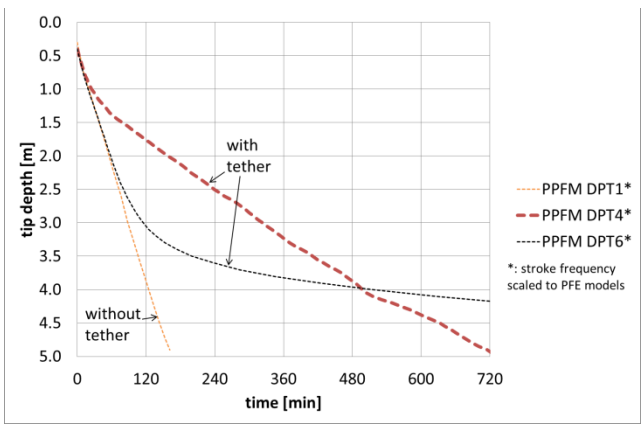

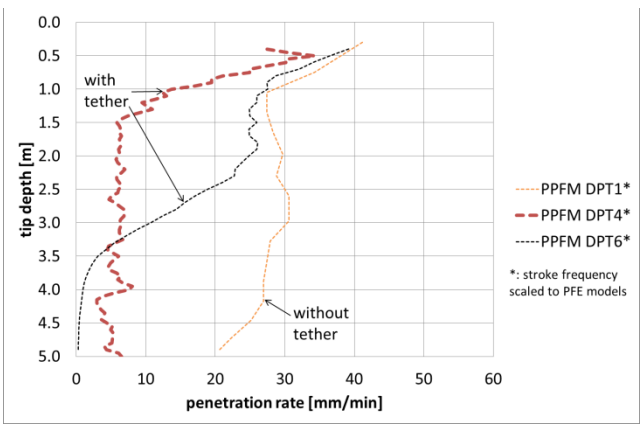

Figure 10: Comparison of PPFM DPTs in quartz sand with (DPT6) and without tether (DPT1) and in Syar with tether (DPT4) - depth over time (left) and depth over penetration rate (right)

In the PPFM DPT6 the external shape was exactly the same as for a PFE model and a Science Tether was installed. The recorded data shows very similar results for the section between start and 2.0 m. Afterwards the knee in the PPFM DPT6 curve starts, which does not appear in the DPT1 test. There the penetration rate remains relatively constant at approx. 28 mm/min and only below 4.1 m it drops slowly to 20 mm/min. This indicates that a knee in the tip depth over time curve might start here.

2.4. Penetrometer measurements

For early DPTs, characterization of the soil and its variation amongst different tests was attempted with the hydraulic cone penetrometer HYSON 100 kN – LW, of the manufacturer A.P. van den Berg (shown in Figure 11). The hydraulic device uses a segmented rod to push an instrumented cone into the soil which measures pressure to overcome penetration resistance and side friction. The tip resistance is calculated by the force on the cone tip (measured by the penetrometer) divided by its cross section. The friction measurement was not useful for this application, as this only gives reasonable values for soils with significant water content. The water content in the used soils for the DPTs was negligible.

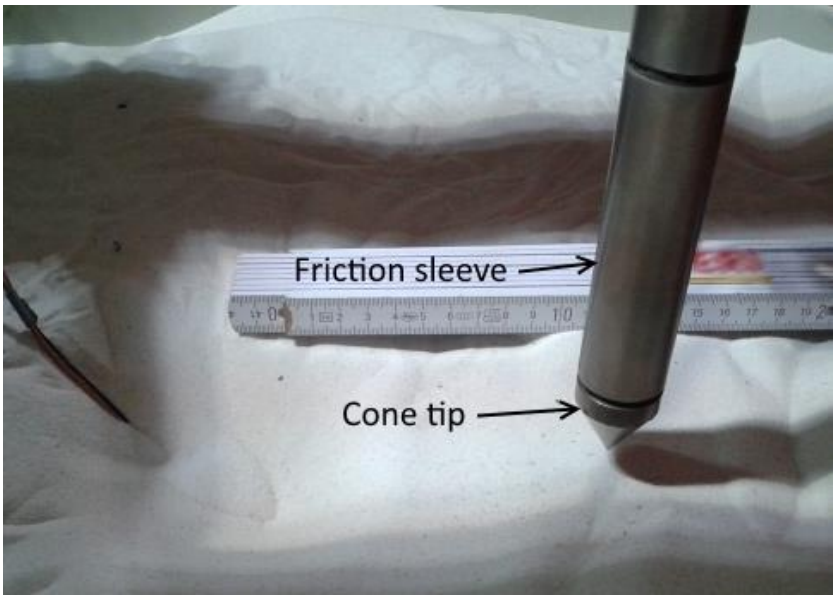

Figure 11: Penetrometer - instrumented cone

Two example measurements for the tip resistance in comparison to the Mole penetration rate can be seen in Figure 12 and Figure 13. A schematic, to explain the measurement locations, is shown in Figure 14; the prefix Pre and Post determine whether the measurement was done before or after the deep penetration test. In the results of the PFE-1 DPT2 test (Figure 12) a significant increase in the tip resistance values after the DPT can be observed and the curves follow a similar trend then the penetration rate, although inverted along the x-axis. Additionally all penetrometer measurements taken in 300 mm from the center of the testbed show partially lower tip resistance values than their corresponding measurements closer to the center in the same direction. This shows an influence from the Mole testing, mostly near the center. In PFE-1 DPT3 (Figure 13), on the other hand, such an influence cannot be completely described. Only in parts is a similar tendency observable. As such measurements were more usual than the results shown in Figure 13, a reliable correlation between tip resistance, soil compaction and Mole performance could not be established. The reasons for the different penetrometer results were not investigated in detail up to this point. Later DPTs skipped this measurement to conserve limited time and personnel resources.

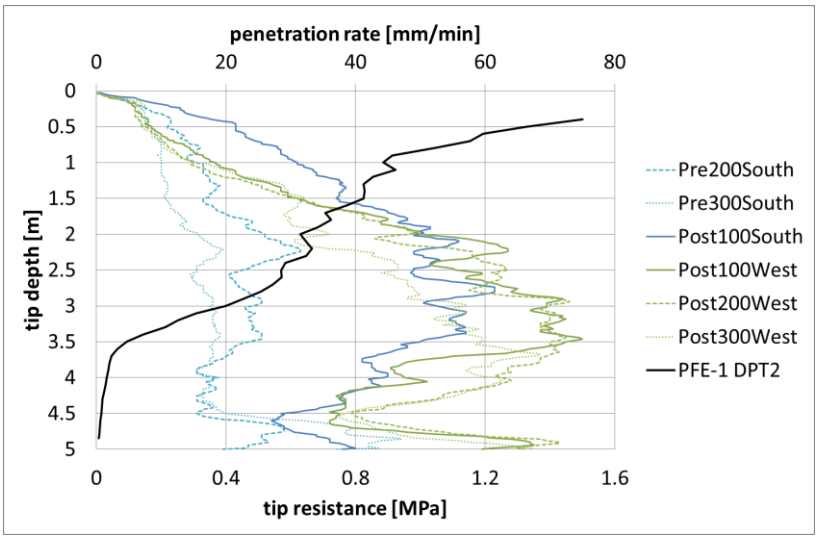

Figure 12: Tip resistance measurements of the penetrometer - prior to the PFE-1 DPT2 test in quartz sand (bright lines) and after the test (dark lines). Depth over penetration rate curve of PFE-1 DPT2 (black line) for comparison.

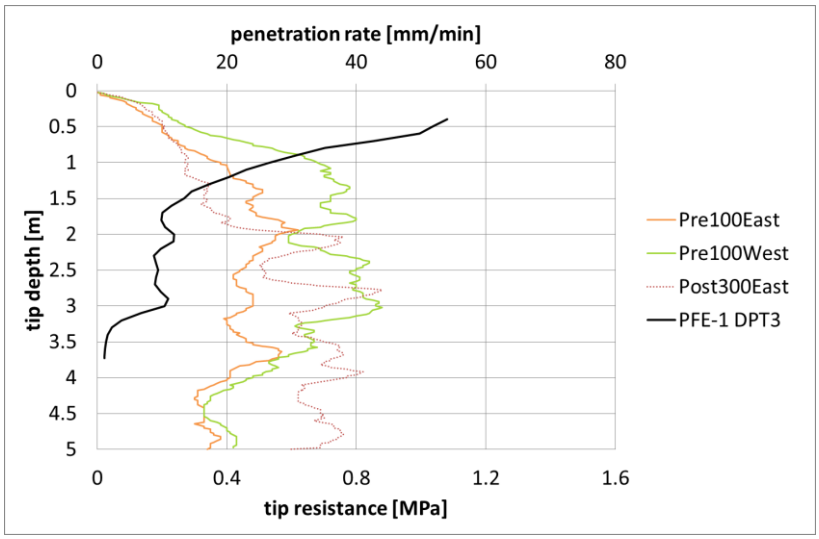

Figure 13: Tip resistance measurements of the penetrometer - prior to the PFE-1 DPT3 test in quartz sand (bright lines) and after the test (dark line). Depth over penetration rate curve of PFE-1 DPT3 (black line) for comparison.

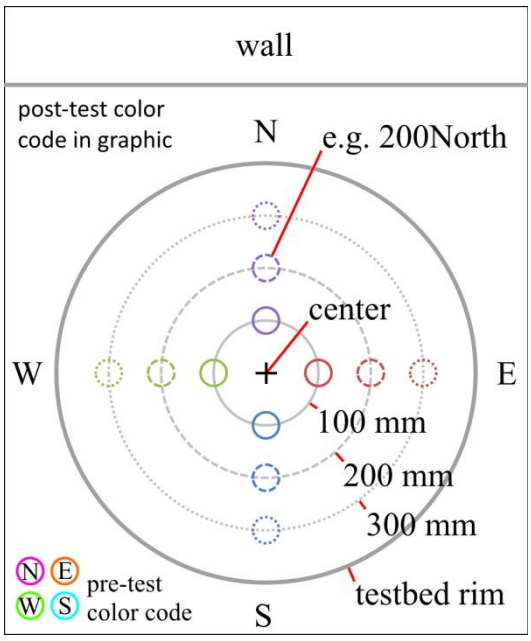

Figure 14: Location of the penetrometer measurements in the testbed: Curve identifiers consist of time of measurement (pre- or post-test), distance from the center (100, 200 or 300 mm) and direction (North, South, West or East). Compare position of the wall with Figure 7.

During some of the later DPTs, when the penetrometer measurement was performed after the test, a localization system, based on three arrays of microphones, was used to roughly determine the position of the Mole inside the testbed prior to the post-test penetrometer measurement. Since the penetrometer cone is pushed into the soil with up to 10 kN, a collision of the cone with the Mole or the Science Tether had to be excluded.

2.5. Test interpretations

In general more deep penetration tests are necessary to broaden the database and proof the theories and interpretations of the data in this section. For indications that certain effects have at least a significant influence on the Mole penetration performance the test results presented are considered sufficient.

1. Tether friction force for depths below 2 m:

As the major difference between the PPFM DPT6 and PPFM DPT1 tests in 2.3.3 is the flat ribbon Science Tether, resp. the steel rope with wires during DPT1, the results suggest that the Science Tether has a big influence on the penetration performance for depths below 2 m. The most influential parameter could be the friction force between cable (flat ribbon or round wire/steel rope) and the soil.

The normal force F_n is calculated by the internal pressure of the soil on the cable p_s and the surface area of the cable in contact with the soil A_c. As the internal pressure is varying depending on the depth of the soil column, the local normal force is the product of the pressure, current depth l and surface area per length A_c/l. The total normal force is then the integral of pressure and surface area per length over the depth at the current depth. The friction force F_f on the cable is calculated with the coefficient of friction μ_s, the surface area per length A/l, the length of cable inside the soil l, and the internal pressure of the soil p_s, which scales with gravity.

$$F_f(l) = \mu_s * \frac{A_c}{l} * \int_{z=0}^{l} p_s(z)\, dz$$

The surface areas per length in soil of the cables are given in

	PPFM DPT1		PPFM DPT6
Cable	Steel rope	Round wires	Flat ribbon
Surface material	Stainless steel	PVC	Polyimide
Coefficient of friction for sliding on same material	0.76	0.40	0.48
Surface area per cable length	12.6 mm²/mm	6.3 mm²/mm	72.4 mm²/mm
Product of COF and surface area per length (sum of both cables for DPT1)	12.1 mm	12.1 mm	34.8 mm

Table **4**. To compare the coefficients of friction for the used materials, their coefficients for sliding against themselves are listed in

	PPFM DPT1		PPFM DPT6
Cable	Steel rope	Round wires	Flat ribbon
Surface material	Stainless steel	PVC	Polyimide
Coefficient of friction for sliding on same material	0.76	0.40	0.48
Surface area per cable length	12.6 mm²/mm	6.3 mm²/mm	72.4 mm²/mm

Product of COF and surface area per length (sum of both cables for DPT1)	12.1 mm	12.1 mm	34.8 mm

Table **4**. For an approximate qualitative comparison of the two cables, those coefficients are sufficient. The internal pressure is a function of the weight of the soil column resting on top of the current layer. The weight is in turn a function of mass distribution, gravity and height of soil column. The mass-distribution of the soil and gravity are (approximately) the same for both tests. Therefore the internal pressure in this case is ultimately a function of the height of the soil column, which is equal to the length of cable in the soil l, the friction angle of the soil and the compaction caused by the Mole penetration. The pressure therefore changes approx. the same way for PPFM DPT1 and PPFM DPT6, which were both performed in quartz sand. The difference in the friction force for both tests is therefore the product of the coefficient of friction and the surface area per length.

	PPFM DPT1		PPFM DPT6
Cable	Steel rope	Round wires	Flat ribbon
Surface material	Stainless steel	PVC	Polyimide
Coefficient of friction for sliding on same material	0.76	0.40	0.48
Surface area per cable length	12.6 mm^2/mm	6.3 mm^2/mm	72.4 mm^2/mm
Product of COF and surface area per length (sum of both cables for DPT1)	12.1 mm	12.1 mm	34.8 mm

Table 4: Physical properties of the cables used in PPFM DPT1 and DPT6

The resulting products cannot be used for a quantitative calculation of the friction force. But for the comparison of the friction forces for the two tests, these values give an impression of the order of magnitude in difference in the friction forces. When put in relation to each other the friction force on the Science Tether in DPT6 is approx. 3 times higher than on the cables in DPT1, for the case of the collapsed borehole. As the width of the Science Tether is higher than the diameter of the Mole, in a nominal case the "cutting" of the tether through the soil is causing the borehole to collapse. The test results seem to be in line with this theory and indicate a major influence of the cable friction forces on the penetration performance for depths below 2m in quartz sand, causing the knee in the nominal DPTs in WF34.

2. Soil properties:

As already discussed in 2.3.2 for the Syar soil, the knee at approx. 3 m depth is not present in the PPFM DPT4 test. When comparing this test with the DPT1 test in Figure 10, some similarities can be observed. Both tests have a steep decrease in penetration rate in the first part of the test and a relatively steady penetration rate afterwards. The test in Syar has that turnover later at 1.5 m and reaches lower penetration rate values than the DPT1 test (turnover at 1.0 m). This could lead to the conclusion, that the friction force on the cable in Syar was also relatively low. As a Science Tether was part of the setup in DPT4 as well as in DPT6, the only difference here is the soil. The soil properties and the compaction of the soil the Mole is capable to cause.

In a high cohesive soil like Syar, the soil particles are more likely to be supported by other particles around them. This leads on one hand to a deeper uncollapsed bore hole (as can be observed in the video of the PPFM DPT4 shown at NASA, 2014). Over that depth the particles cannot apply a force on the Science Tether. On the other hand are the particles, which collapsed into the bore hole and are in contact with the Science Tether, also supported by other particles. So those particles are applying less force to the Science Tether as cohesion-less soil. This could explain the absence of the knee at around 3 m depth.

This interlocking behavior of high cohesive soil is disturbed near the Mole tip by its hammer strokes. A higher local compaction of the Syar soil in comparison to the quartz sand is the result, which was also observed when investigating the soil after a deep penetration test (e.g. emptying the testbed). This is the most likely explanation for the smaller penetration rates after the first knee around 1.5 m.

3. Penetration rate for depths between 1 m and 3m in quartz sand:

The tests in quartz sand seem to show a penetration rate dependent effect for medium depths. One possible explanation could be that the compaction of the soil around the Mole for a relatively narrow band of displacements per stroke (and therefore the penetration rate) is improving the Mole penetration performance, at least for quartz sand WF34.

If it is assumed that the local compaction of the soil due to a single stroke is higher when the displacement due to this stroke is lower, a locally higher internal soil pressure can be expected for cohesionless and therefore uncompressible soils like quartz sand. As a higher friction force on the side walls of the Mole is improving its performance, the penetration rate increases. This effect is limited by the same compaction of the soil that also appears below the tip of the Mole. If the compaction of the soil is too high, the amount of soil the Mole is able to push aside is reduced. On the other hand, if the Mole is progressing too fast, meaning there are less strokes needed to penetrate through the soil over one Mole length, the compaction of the soil around the Mole cannot increase as much as with lower penetration rates. Altogether this would suggest an optimal penetration rate the Mole would naturally show after the higher penetration rate of the start has settled down.

When comparing this model with the curves in Figure 8, the way the three groups of DPTs approach the optimal penetration rate differs significantly. The values for this penetration rate also differ between tests, although a tendency within a group can be seen. One possible explanation for the general trend of the curves can be that the soil-Mole interaction works similar to a mass-spring-damper system. The first group with low penetration rates would have a low spring rate and a high damping ratio, the second group (medium penetration rate) a low spring rate and a low damping ratio and the third group (high penetration rate) a high spring rate.

If such a system exists and what is influencing the optimal penetration rate, cannot be said with the current database. More tests and a better correlation of soil and Mole characterizations to the test results are required in order to validate or disprove this model. It cannot be excluded that a similar effect is also present in high cohesive soils like Syar. The one dataset showing a relatively constant penetration rate over depth (PPFM DPT4) shows a similar trend in the depth vs. penetration rate curves as the PFE2 DPT1 test in quartz sand until 2.6 m depth (see

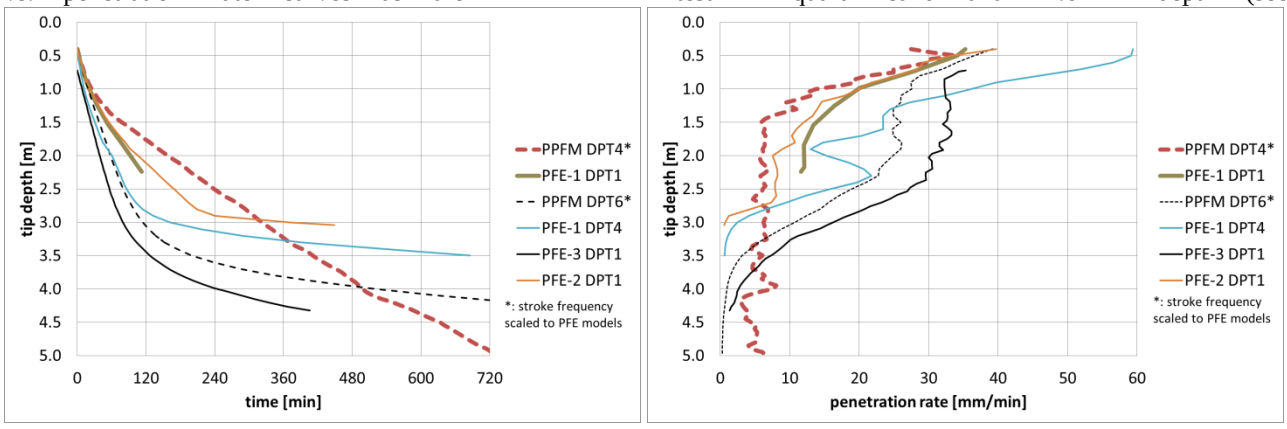

Figure **9**).

3. Full Functional Test

The full functional tests (FFT) were performed to verify that all subsystems are operational and their data show the expected results. Furthermore the performance of the hammering mechanism was measured with a device specifically designed for this purpose – the Mole dynamometer. The dynamometer was also used to confirm that the performance of the Mole after its life test was still in the specified limits.

3.1. Mole Dynamometer

During the early phases of the HP³ development a simple device, developed by DLR, was used to measure the excitation of a spring caused by the Mole strokes, the health check test stand (HCTS). This method was able to show the qualitative differences of the same Mole before and after a test and could be used to qualitatively compare different Moles of the same design. Due to limited device accuracy, quantitative results were not possible with the HCTS. Therefore a new device, called the Mole Dynamometer or "Dyno", was developed and built by JPL and it measures the output force and displacement more directly. This allowed for quantitative results and better experimental repeatability. In this device (shown in Figure 15) the Mole is installed horizontally on a movable sled. When the Mole hammers, the sled is displaced in response to a hammer stroke, moving on cylindrical rails towards a massive block (top left corner in Figure 15) that is rigidly attached to the Dynamometer base plate. The dynamometer measures the force of each stroke with a load cell (model Kistler 9021A) mounted behind a Teflon receiving collar (white cylinder in Figure 3) that is part of the sled. Displacement of the sled in response to a hammer stroke is measured in both forward and reverse directions simultaneously with two linear potentiometers. A typical set of results from a dynamometer measurement procedure is shown in Figure 16. Output quantities as a function of experiment time are: stroke force (for 60 –90 strokes), displacements in the forward and reverse directions (to check for forward motion vs. rebound), and the difference between the two displacement measurements (diagnostic of, for instance, slippage in the Mole clamping). In practice,

only the stroke force was used as an indicator of the Mole performance. Data acquisition rates up to 25 kHz allow every individual stroke to be analyzed in more detail as well (see Figure 16).

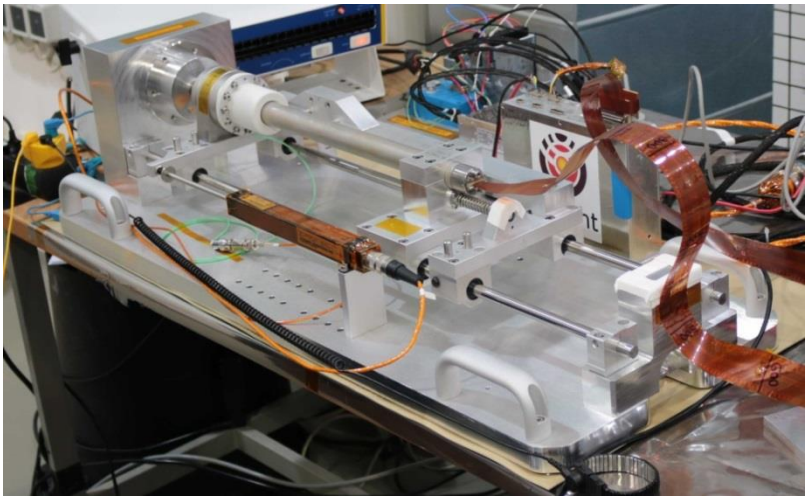

Figure 15: The dynamometer with an installed Mole and a BEE in the background

The Mole dynamometer was used before and after each performance test of the proto-flight equivalent models (PFE) to track the health of the hammering mechanism.

The dynamometer is designed to allow three different test configurations. The setup used for a normal functional test has a relatively soft spring installed between the massive block and the sled. During the operation of the Mole, the spring is compressed until the Mole cannot compress it further, simulating the increase in penetration resistance as the mole reaches greater depth in a relatively uncompacted soil. Reaching this point in the soft-spring configuration normally takes 60 – 90 strokes. Another setup uses a stiff spring in several stages of pre-compression. This strong-spring configuration simulates compacted soils and still greater depths. The third configuration does not use a spring at all, but fixes the sled against the massive block with a rigid aluminium spindle. This "stall" configuration has the Mole hammering against an immovable obstacle, simulating the mole encountering a solid rock in the soil. The strong-spring and stall configurations are used to characterize Mole behaviour in highly stressing cases. As these setups are more demanding for the hammering mechanism and structural parts, the test is normally only performed once and with only ten strokes per setup. The soft-spring setup is less stressing and is used more frequently in the testing campaign.

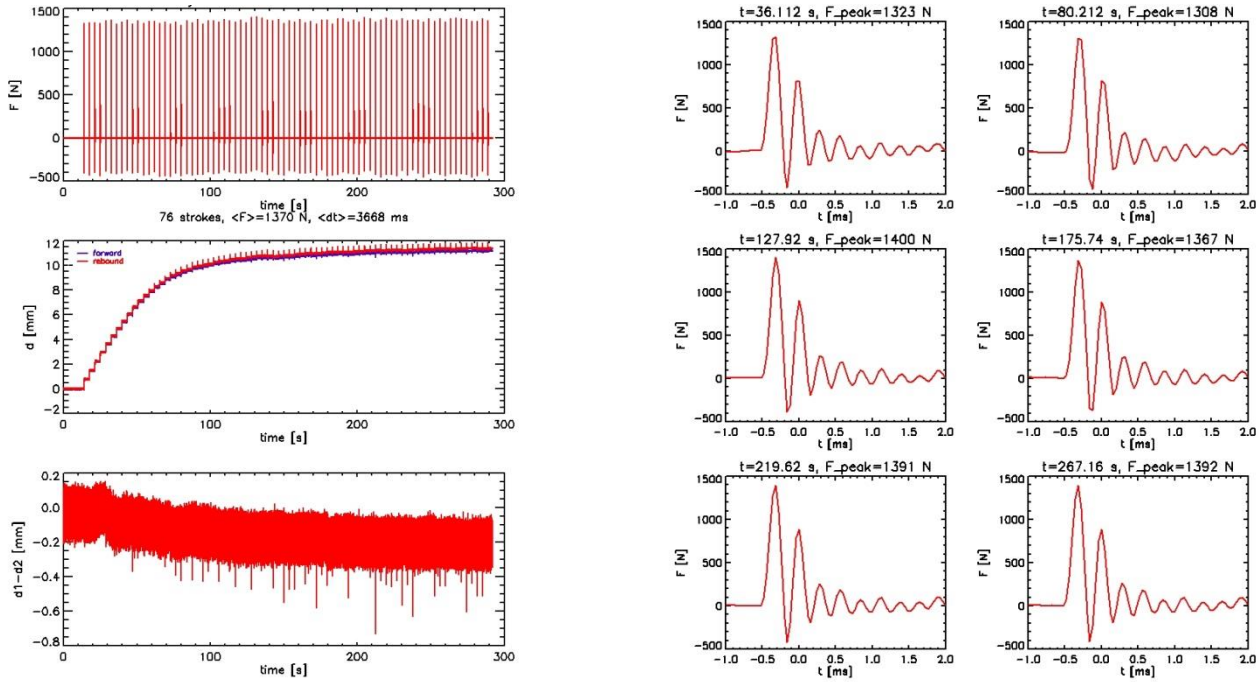

Figure 16: Complete set of results of dynamometer measurement of the PFM-3 Mole (left): force measurement of load cell (top), displacement measurement with potentiometers (middle) and difference of potentiometer measurement between the two sides (bottom). Examples of single-stroke force profiles (right; stroke times and peak forces indicated at the top of each subfigure) recorded by the dynamometer load cell for the PFM-3 Mole.

3.2. Test results

During a full functional test, a BEE records all available subsystem data. For the Mole this dataset consists of the STATIL output values, the TEM-A and TEM-P temperatures, the motor current, the motor temperature sensor and the housekeeping (HK) data in general. The activation of the components is recorded in HK data. After an FFT was performed, the generated data set is sent to the responsible personnel for each functional component for analyzing.

One of the most notable results from the dynamometer is the run-in time of the hammering mechanism. This is a phenomenon where a new built or long-stored Mole shows worse performance during the first strokes. Over the course of approx. 5 to 60 strokes, the stroke force increases until it reaches a steady-state range: its nominal stroke force. Within this range, the precise number of strokes to pass the run-in-time is different for every Mole model. Relatively small differences in models can affect this (e.g. a microscopic burr near a sliding surface can influence the run-in-time). In Figure 17 several dynamometer measurements are displayed, where this effect was observed. The effect seen in long-stored but previously run-in moles is believed to be due to small drifting of parts and lubricants in the mechanism during storage, that need to rectify within the first strokes. Although already observed during the early phases of the project, the dynamometer quantified this effect for the first time.

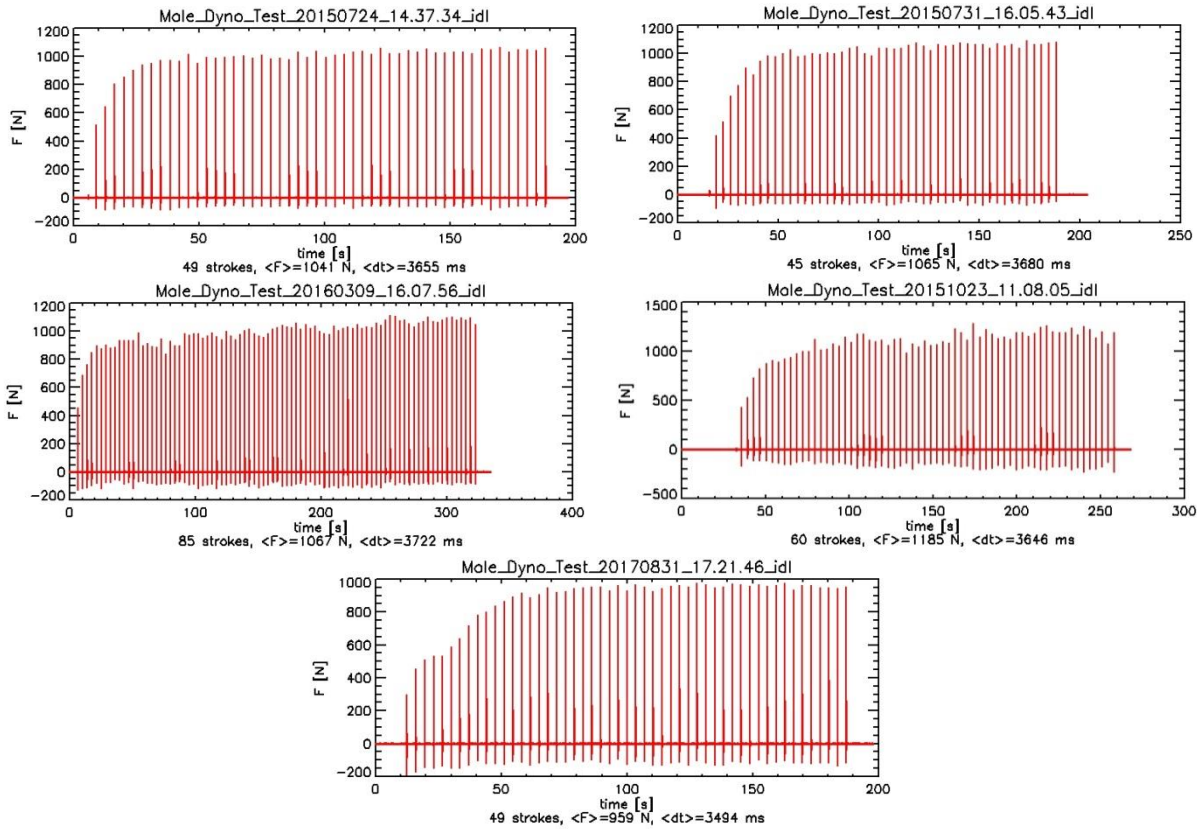

Figure 17: Dynamometer measurements of Mole functional tests with run-in time. Top left: PFE-3 Mole FFT1 (first functional test); top right: PFE-3 Mole FFT2; mid left: PFE-3 Mole FFT8; mid right: PFM-2 Mole FFT1; bottom: PFM-3 Mole FFT10

Following run-in strokes, the nominal stroke force for the flight models and the proto-flight equivalent models is typically between approx. 1000 N and 1200 N. For the stall measurement, the forces were usually measured to be higher, ranging from approx. 1200 N to 1400 N. During the course of all activities with those models, no significant performance drop could be observed. Figure 18 shows the stroke forces of the QM Mole before and after the life test performed for the 2017 flight model.

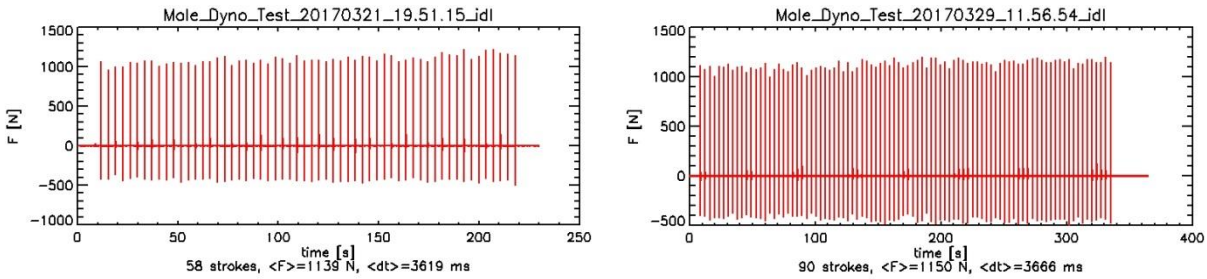

Figure 18: QM Mole force data recorded before (left) and after (right) its life test

4. Further Mole Performance Tests

Apart from the aforementioned tests, a series of other performance and long duration tests were performed with the Mole in different regolith columns or test stands. These investigated Mole penetration behaviour when encountering obstacles and the durability of the components for life testing.

4.1. Life Cycle Test (also called 'Mechanism Life Test')

During the qualification of the HP³ Mole, one of its major challenges was the life cycle test. The goal of the test was to operate the hammering mechanism in a representative Mars environment for three times the estimated duration to reach 5 m depth. Based on deep penetration tests with the PFE models the total stroke count was set to 6,500 for a single life and 19,500 for the required three life times (rounded up to 20,000 in the life time requirement L5-TM-3) with a qualification model (PFE-3 for the PFM-1 flight model and QM for the PFM-3 flight model; see Table 2). The specific environmental conditions that represent the martian subsurface at the InSight landing site are ambient pressures of 6 mbar CO_2 and a regolith temperature of approximately -55°C (though to provide testing margin, lower temperatures down to approximately -70°C were employed). To realize this simulated Mars environment, the Geothermal Testbed at JPL was initially planned to be used for this purpose (shown in Figure 19). A detailed description of the geothermal testbed is compiled by Smrekar et al. (2012).

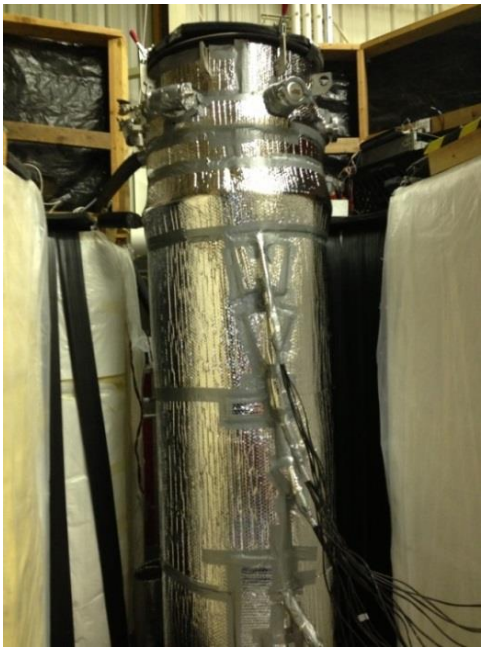

Figure 19: The JPL Geothermal Testbed with opened insulation and platform (described in Smrekar et al., 2012)

As the delivery of the life test unit of the Mole, PFE-3, to JPL was delayed and technical problems occurred with the Mole shortly after it started its first life test attempt, the full life test could not be finished on time for the flight model PFM-1. Thus a different approach was developed to conduct a faster life test at DLR after refurbishment of the PFE-3 model.

4.1.1. DLR Life Test Campaign

In order to realize a test setup that is similarly demanding then penetrating into soil under Martian environmental conditions and is faster to conduct, the life test was conducted in a climate chamber and in a test stand. The test stand was the health check test stand (mentioned in section 3.1), where the Mole is hammering against a spring to simulate a reaction force for the strokes similar to hammering against soil. This test stand does not require a reset during usage, though enabling continuous testing and accumulating the stroke count as fast as possible once the test was started. For the Martian environment a compromise had to be made. As one can expect, the low temperatures have a significant influence on the components such as solder and wires which will become more brittle and were usually the parts that caused a malfunction in previous tests. Additionally the performance of lubricants is affected by low temperatures. The actual Life Tests with the HP³ Mole were conducted in this climate chamber at a relevant temperature.

After approximately half the stroke count, the Mole was taken out of the climate chamber and a DPT was conducted to show the penetration performance in soil as well. Between each of those test blocks an additional FFT was performed to check for degradation in the stroke force output of the tested Mole and functionality of the other subsystems.

4.1.2. Test results

During the first life test with the PFE-3 Mole, which is equal to the PFM-1 Mole the fault protection of the BEE engaged due to an open temperature sensor line, after approx. one lifetime. In order to fulfil the number of strokes first and discuss the consequences afterwards, this fault protection was turned off. During the remaining part of the test two other components malfunctioned. However, none of the failed components affected the Mole's ability to hammer. As for all lost components other sensors could be used to fulfil all required measurements, the test was partially passed. At that time the PFM-1 flight model was already built. But also the launch of InSight was postponed to 2018. With the results of the first life test and the additional time available, the design of the Mole was improved.

For this updated design two new Mole models and one new Support System flight model were built and tested. The second life test with the QM model was conducted before the new flight model integration of the PFM-3 model started and the life test was passed without anomalies. Due to shifts in the schedule of this project, the QM Mole performed 6 lifetimes worth of strokes with approximately 5 lifetimes (3 lifetimes with a Science Tether coupon) under cold temperature and one lifetime hammering in soil under ambient conditions.

4.2. Low pressure penetration tests

After the first protoflight equivalent model with the new hammering mechanism was integrated, a new test campaign was added to investigate the Mole penetration performance under low, Mars-like, pressure. The purpose was to have a first estimate of the penetration behavior of the Mole in the GTB before sending the Mole to JPL. Due to the simplifications of this test setup compared to the GTB tests, faster test runs and different test configurations could be realized.

For this test a small bin (diameter of 400 mm and height of 700 mm) filled with soil and with the PFE-1 Mole inserted into the soil (either by hand or by hammering in ambient conditions) was put in a vacuum chamber. The chamber was evacuated to approximately 1 mbar and kept there for a longer period to allow enclosed gas inside the soil to escape. Afterwards the pressure was increased to 6 – 10 mbar and the hammering was started. A change of the compaction of the soil due to the evacuation could not be observed.

The first test run in Syar, where the Mole was placed inside the testbed by hand, was not successful. The Mole was penetrating downwards as expected, but stopped to progress shortly afterwards. After some additional hammering time at the same location, the Mole then started to slowly retract out of the soil. To understand this anomaly, different test configurations were tested as well. The following parameters were changed one by one while leaving the other conditions unchanged during this investigation:

1. Test medium: Syar and quartz sand
2. Mole insertion method: pushed in by hand and Mole operated insertion
3. Different atmospheric pressures: 6 – 10 mbar, ambient and increments in between

An overview of all test runs and their results is listed in Table 5. The results can be summarized as followed:

- The method of insertion does not seem to impact the penetration during these tests
- All tests with the cohesion-less quartz sand were successful, independent of the pressure
- Tests in the high cohesive Syar were successful above a threshold of approximately 70 to 100 mbar

Pressure		6 – 10 mbar	Intermediate	Ambient
Quartz sand	Hand inserted	successful	Not tested	successful
	Mole operated	successful	Not tested	successful
Syar	Hand inserted	Not successful	Successful at 70 – 100 mbar and above	successful
	Mole operated	Not successful	Not tested	successful

Table 5: Overview of test results in the low pressure test campaign conducted with the PFE-1 Mole

To rule out an impact of the low pressure on the hammering mechanism operations, the PFE-1 Mole was operated in a high-speed x-ray device under low pressure. There, no change of the mechanism dynamics was observed.

In a second campaign the tip of the Mole was modified. Here a ring of barbs around the tip should reduce, if not prevent the backwards movement of the Mole inside the soil. But at least with the realized short term solution the hammering in Syar under low pressure was still not successful. As the addition of the barbed tip on this model did not improve the issue, it was disregarded for further use. At the time when the anomaly occurred, was investigated and first minor changes to the design could not improve the performance of the Mole, the decision had to be made that the tight schedule of this project does not allow a more in-depth solution.

Analysis of the expected soil in the landing site area suggested that the InSight mission would land on regolith with very low cohesion, as described by Golombek et al. (2017) and that quartz sand would be more representative of the Martian regolith than Syar. Due to the very constrained time left until launch, the difficult decision had to be taken to carry on with the project without completely solving this issue. As a consequence, Syar was dropped as a test medium and only penetration tests in quartz sand were conducted from this point onwards.

Still, analysis suggested two possible root causes for the failure to penetrate in Syar at low pressure. First, imperfect evacuation of the Syar may have caused some gas overpressure in the sand. Second, a detailed force balance suggested that a "suction" effect should matter. When the Mole starts to recoil, it will have to open a cavity at its tip against the pressure exerted by the atmosphere. At Earth atmosphere pressure that force will be significant, at low pressure the force will be too small to be effective. The "suction" effect would explain why the Mole penetrates even in cohesive soil at Earth atmosphere pressure. For cohesionless sand the suction effect would not be as important due to the friction on the hull provided by the soil. Apart from the cohesion, other effects that may have contributed to the failure to penetrate are the wide particle-size distribution and the large friction angle of Syar.

An about 10cm thick highly cohesive duricrust has been observed at the site of the Mole on Mars. The low friction provided by the crust is considered to be the most likely root cause for the currently experienced penetration anomaly of the HP³ Mole operations (status of September 2019). However, other root causes such as a rock of a size too big for the Mole to push aside cannot (yet) be ruled out (Spohn et al., 2019).

4.3. Deflection Test

During the deflection test, the BBM Mole would penetrate vertically downwards in a 1 m x 2 m x 2 m (W x L x H) bin filled with WF-34 quartz sand until it hit a 50 mm thick 400 mm x 400 mm concrete plate which was put into the soil at an angle. The Mole was positioned to hit the plate approximately in the center. This test was performed for plate angles of 20°, 40° and 50°, where 0° would be vertical. The BBM Mole had a STATIL installed, so that its orientation was recorded. The depth was measured with markings on the Science Tether.

For the test run with the 20° angle, the Mole was deflected and it changed its orientation to be parallel to the plane of the concrete plate and it continued its course along this plane. After passing the plate the Mole continued progression in the new orientation. The test was not performed long enough afterwards to observe any change to the vertical orientation. Other early tests with the Mole showed its capabilities to reorient itself along the gravity vector. At a plate orientation of 40° from vertical, the Mole was still deflected, but did not change its orientation. It scratched the concrete plate significantly while it pushed itself sideways through the soil along the plane of the plate. At a plate orientation of 50° from vertical, the Mole was not deflected but stayed at one spot on the concrete plate and started excavate a small cavity into the plate. The test was aborted after several hours of no vertical progress. After the excavation of the concrete plate the hole was measured to be approx. 5 mm deep. Table 6 gives an overview of the test results.

Plate angle	20°	40°	50°
Mole deflected	Yes	Yes	No
Mole orientation changed	Yes	No	No
Test passed	Yes	Yes	No

Table 6: Overview of test results of the deflection test

These test results indicate the capability of the Mole to deflect around smooth obstacles at angles up to at least 40 degrees from vertical. Although on Mars smooth rocks are less likely, this size rocks is also unlikely to be found in the landing site area as described by Golombek et al. (2017).

4.4. Layers Test

An early test in 2012 showed the capability of the MMM Mole to penetrate through different layers of soil and other obstacles. Those layers consisted of Mojave Mars Simulant (MMS) dust (from surface to 0.98 m depth; see Table 3), rocks (from 0.98 m to 1.05 m depth) and MMS sand (from 1.05 m to 2 m depth) and are shown in Figure 20. To prevent mixing of the curated mars regolith sands and dusts, an unperforated layer of paper was emplaced at 0.98 m depth between the rock layer and the dust layer. The rocks, seen in Figure 21, were composed of fracture-resistant Columbia River basalt and ranged from 5 to 15 cm in size. These were arranged in a mosaic pattern which had no gaps larger than the diameter of the Mole. In the penetration curve (see Figure 22) the reduction in penetration performance as the Mole approached the paper and rock layers can be seen. Both the paper and the rocks acted as a barrier to regolith motion (similar to the wall effects described above) and therefore to Mole progress. Nevertheless, after a temporary slowdown the Mole successfully penetrated through all layers.

Figure 20: Different layers for the layers test: MMS dust (top left), paper (top right), rocks (bottom left) and MMS sand (bottom right)

Figure 21: Rock sizes in comparison to a human hand

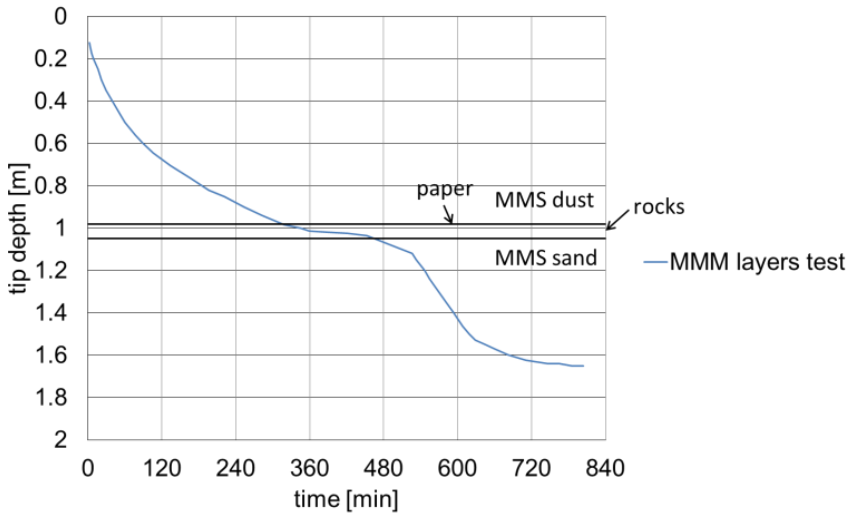

Figure 22: MMM Mole tip depth over time

The maximum hammering forces that could be achieved with the MMM Mole and the BBM Mole hammering mechanisms are significantly less than the later PFE/PFM/QM hammering mechanism designs. The installed force springs in the MMM and BBM models had a lower spring rate and work range as the later models, thus the potential energy of the hammering mass inside the mechanism was significantly lower. Since the tests of layer penetration and obstacle deflection were successful with even these earlier prototypes, a repeat of the tests with the more capable Moles was deemed unnecessary.

This test indicate that the Mole is capable to push itself past small sized obstacles of up to 100 mm and probably past bigger obstacles till 150 mm as well (Golombek et al., 2017). Those results were taken into account for the landing site selection of InSight. The Mole here has a chance of 43% for a depth of 3 m or 59 % for 5 m to encounter a rock that will stop the penetration in the most pessimistic scenarios. Depending on the actual rock abundance at the landing site, this chance can get down to a relatively low value of 2% for a depth of 3 m or 10 % for 5 m (Golombek et al., 2017 p. 78).

5. Summary and Conclusion

During the course of HP^3 development as part of the InSight project and also during the preparation before that, a number of tests were conducted to estimate the performance and capabilities of various Mole models. The full functional tests were useful to monitor the integrity of the hammering mechanism and other subsystems within the Mole. While those tests normally did not result in new findings, some tests showed malfunctions that required maintenance or even design changes.

In a variety of performance tests the Mole showed its capabilities to operate for sufficient duration, including margins, and to overcome small obstacles. But also the limitations for the Mole were found. So bigger sized rocks (15 cm and above) can lead to a sudden halt in the penetration. Furthermore, a cohesive soil at the deployment site, similar to Syar,

can lead to a ceasing progression even early in the penetration phase. But as described by Golombek et al. (2017) the risk for those two cases is relatively small.

The deep penetration and geothermal tests showed that the Mole is capable to reach its targeted depth. But additionally the Mole-soil-interaction was better understood during the test campaigns conducted in this project. The self-compaction caused by the Mole and the resulting impact on the penetration performance was well known before and served as a baseline for models for the penetration performance of the Mole as described by Poganski et al. (2017). The additional effects caused, presumably, by the tether friction below 2 m and an optimal penetration rate at depths between 1 and 3 m can be a reasonable explanation of the additional tendencies found in the results. A broader database, especially with different soils, could give more evidence towards some of the ideas presented in this paper. But due to the focus of getting the hardware ready to be sent to Mars, not all scientifically interesting aspects could have been investigated in detail during the course of this project.

6. Acknowledgements

For the development and testing in Germany of the HP³ Mole, funding was granted by German Aerospace Center DLR "Programmdirektion Weltraum" in support of the HP³ instrument for the InSight mission. This work was a multi-DLR center effort and carried out at DLR's Institute of Space Systems in Bremen, Germany.

For the development of the Dynamometer, the GTB testing and further Mole penetration testing (e.g. the layers test), funding was granted by the Jet Propulsion Laboratory, California Institute of Technology, Pasadena, USA, under a contract with the National Aeronautics and Space Administration in support of the HP³ instrument for the InSight mission.

7. References

W.B. Banerdt, S.E. Smrekar, P. Lognonné, T. Spohn, et al. (2013). *InSight: A Discovery Mission to Explore the Interior of Mars*, Lunar Planet. Sci. Conf. (Lunar and Planetary Institute, Houston, 2013), Abstract #1915.

M. Golombek, D. Kipp, N. Warner, I.J. Daubar (2017), *Selection of the InSight Landing Site*, Space Sci. Rev, 211(1-4), 5-95. https://doi.org/10.1007/s11214-016-0321-9

M. Grott, J. Knollenberg, C. Krause (2010), *The Apollo Lunar heat flow experiment revisited: A critical reassessment of the in-situ thermal conductivity determination*, J. Geophys. Res., 115 (E11). https://doi.org/10.1029/2010JE003612

R. Lichtenheldt, O. Krömer (2016), *Soil Modeling for InSight's HP³-Mole: From Highly Accurate Particle-Based towards Fast Empirical Models*, Earth and Space 2016: Engineering for Extreme Environments, ed. by R.B. Malla, J.H. Agui, P.J. van Susante (ASCE Library, Reston, 2016), p. 142-153. https://doi.org/10.1061/9780784479971.016

NASA (2014), *Time lapse of the HP3 'mole' – NASA's InSight Mars Lander*, retrieved 15. November 2018 from https://mars.nasa.gov/resources/22080/time-lapse-of-the-hp3-mole

NASA/JPL-Caltech (2018), *The InSight Lander – NASA's InSight Mars Lander*, retrieved 13. November 2018, from https://mars.nasa.gov/insight/multimedia/images/2018/the-insight-lander

J. Poganski, N.I. Kömle, G. Kargl,.H.F. Schweiger, et al. (2017), *Extended Pile Driving Model to Predict the Penetration of the Insight/HP3 Mole into the Martian Soil*, Space Sci. Rev 211(1-4), 217-236. https://doi.org/10.1007/s11214-016-0302-z

S. Reershemius, M. Fittock, T.L. Hudson, K. Sasaki, et al. (2018), *Structure Development of the HP³ Instrument Support System for the Mars Mission InSight*, pre-print submitted to Acta Astronaut.

S.E. Smrekar, T.L. Hudson, P. Morgan (2012), *Instrumentation for Measuring Lunar Heat Flow*, paper presented at International Workshop on Instrumentation for Planetary Missions, Goddard Space Flight Center

T. Spohn, M. Grott, S.E. Smrekar, J. Knollenberg, et al. (2018), *The Heat Flow and Physical Properties Package (HP³) for the InSight Mission*, Space Sci. Rev, 214:96. https://doi.org/10.1007/s11214-018-0531-4

T. Spohn, S.E. Smrekar, T.L. Hudson, M. Grott, et al. (2019), *The Heat Flow and Physical Properties Package HP³ on InSight – First Results*, 9th Intern. Conf. on Mars (Lunar and Planetary Institute, Pasadena, 2019), Abstract #6163.

Appendix A DPT test data

Model	Test ID	Date	Soil
PPFM	DPT1	20140205	Quartz sand WF34
Insertion method		**Depth recording**	
By hand until initial depth		Via camera and cable marks	
Time [min]	**Time scaled to PFE stroke frequency [min]**	**Tip depth [m]**	**penetration rate [mm/min]**
0.00	0.00	0.30	41.14
5.00	10.94	0.75	34.29
10.00	21.88	1.05	27.43
15.00	32.81	1.35	27.43
20.00	43.75	1.65	28.34
25.00	54.69	1.97	29.71
30.00	65.63	2.30	28.80
35.00	76.56	2.60	30.63
40.00	87.50	2.97	30.63
45.00	98.44	3.27	27.89
50.00	109.38	3.58	27.43
55.00	120.31	3.87	26.97
60.00	131.25	4.17	26.97
65.00	142.19	4.46	25.14
70.00	153.13	4.72	22.35
74.00	161.88	4.90	20.57

Table 7: PPFM DPT1 data set

Note: No flat-wire ribbon cable was installed.

Model	Test ID	Date	Soil
PPFM	DPT4	20140327	Syar
Insertion method		**Depth recording**	
By hand until initial depth		Via camera and ST marks	
Time [min]	**Time scaled to PFE stroke frequency [min]**	**Tip depth [m]**	**penetration rate [mm/min]**
0.00	0.00	0.40	27.44
0.83	1.82	0.45	30.48
1.50	3.28	0.50	34.27
2.17	4.74	0.55	30.13
3.02	6.60	0.60	30.15
3.68	8.06	0.65	27.44
4.68	10.24	0.70	24.93
5.52	12.07	0.75	24.93
6.52	14.26	0.80	21.11
7.68	16.81	0.85	19.45
8.87	19.40	0.90	19.45
10.03	21.95	0.95	17.15
11.53	25.23	1.00	13.71
13.37	29.24	1.05	12.47
15.20	33.25	1.10	13.00
16.88	36.93	1.15	11.38
19.22	42.04	1.20	9.46
21.72	47.51	1.25	10.12
23.73	51.92	1.30	10.93
25.90	56.66	1.35	9.14
28.73	62.85	1.40	7.39
32.08	70.18	1.45	6.36
35.92	78.57	1.50	5.82
39.93	87.35	1.55	6.22
43.27	94.65	1.60	6.36
47.12	103.07	1.65	6.22
50.62	110.72	1.70	6.52
54.13	118.42	1.75	6.21
57.98	126.84	1.80	6.36
61.32	134.13	1.85	6.36
65.17	142.55	1.90	6.08
68.83	150.57	1.95	6.22
72.52	158.63	2.00	5.95
76.52	167.38	2.05	5.70
80.53	176.17	2.10	5.95
84.20	184.19	2.15	6.51
87.55	191.52	2.20	7.01
90.72	198.44	2.25	6.51
94.57	206.87	2.30	5.81
98.58	215.65	2.35	5.82
102.42	224.04	2.40	6.22
105.93	231.73	2.45	6.52
109.43	239.38	2.50	6.08
113.45	248.17	2.55	5.95
117.12	256.19	2.60	5.07
122.47	267.90	2.65	4.71
126.82	277.41	2.70	5.59
130.65	285.80	2.75	6.22
134.17	293.49	2.80	6.84
137.33	300.42	2.85	6.84
140.85	308.11	2.90	6.84
144.02	315.04	2.95	6.36
148.03	323.82	3.00	6.21
151.38	331.15	3.05	6.36
155.22	339.54	3.10	6.22
158.73	347.23	3.15	6.22
162.57	355.62	3.20	6.51
165.75	362.58	3.25	6.67
169.42	370.60	3.30	5.59
173.93	380.48	3.35	4.63
179.28	392.18	3.40	4.49
184.12	402.76	3.45	5.26
187.97	411.18	3.50	6.08
191.63	419.20	3.55	5.47
196.32	429.44	3.60	4.97
200.83	439.32	3.65	4.64
206.17	450.99	3.70	4.64
210.68	460.87	3.75	5.81
214.03	468.20	3.80	6.36
217.87	476.58	3.85	5.95
221.72	485.01	3.90	6.67
224.72	491.57	3.95	8.04
227.40	497.44	4.00	7.60
230.73	504.73	4.05	5.47
235.75	515.70	4.10	3.85
242.60	530.69	4.15	2.94
251.28	549.68	4.20	2.94
258.13	564.67	4.25	3.22
265.48	580.74	4.30	3.55
271.00	592.81	4.35	4.08
276.68	605.24	4.40	3.85
282.87	618.77	4.45	3.60
289.38	633.03	4.50	4.42
293.20	641.38	4.55	5.17
298.22	652.35	4.60	4.97
302.40	661.50	4.65	5.31
315.43	690.01	4.80	5.12
320.27	700.58	4.85	4.03
326.78	714.84	4.90	4.34
330.80	723.63	4.95	6.07
334.32	731.32	5.00	6.50

Table 8: PPFM DPT4 data set

Model	Test ID	Date	Soil
PPFM	DPT6	20160204	WF34
Insertion method		**Depth recording**	
By hand until initial depth		Via camera and ST marks	
Time [min]	**Time scaled to PFE stroke frequency [min]**	**Tip depth [m]**	**penetration rate [mm/min]**
0.00	0.00	0.40	39.17
1.17	2.55	0.50	36.57
2.50	5.47	0.60	34.08
3.85	8.42	0.70	32.08
5.35	11.70	0.80	28.72
7.03	15.38	0.90	27.43
8.68	18.99	1.00	27.56
10.35	22.64	1.10	26.00
12.20	26.69	1.20	26.00
13.87	30.33	1.30	24.93
15.87	34.71	1.40	24.94
17.53	38.35	1.50	26.00
19.38	42.40	1.60	24.82
21.22	46.41	1.70	24.93
23.05	50.42	1.80	26.12
24.72	54.07	1.90	26.00
26.57	58.12	2.00	24.82
28.40	62.13	2.10	23.85
30.40	66.50	2.20	22.86
32.40	70.88	2.30	22.76
34.42	75.29	2.40	21.02
36.75	80.39	2.50	18.92
39.25	85.86	2.60	17.09
42.10	92.09	2.70	15.63
45.10	98.66	2.80	14.40
48.45	105.98	2.90	12.44
52.45	114.73	3.00	10.73
56.97	124.62	3.10	8.82
62.82	137.41	3.20	7.12
69.82	152.72	3.30	5.53
79.35	173.58	3.40	4.31
91.03	199.13	3.50	3.15
108.42	237.16	3.60	2.38
129.47	283.21	3.70	1.86
157.52	344.57	3.80	1.41
194.28	424.99	3.90	1.15
237.20	518.88	4.00	0.98
287.48	628.87	4.10	0.83
346.97	758.99	4.20	0.69
419.78	918.28	4.30	0.59
501.13	1096.23	4.40	0.50
602.23	1317.39	4.50	0.43
713.32	1560.38	4.60	0.37
847.30	1853.47	4.70	0.34
985.15	2155.02	4.80	0.30
1151.22	2518.29	4.90	0.27
1313.47	2873.21	5.00	0.27

Table 9: PPFM DPT6 data set

Model	Test ID	Date	Soil
PFE-1	DPT1	20140812	WF34
Insertion method		**Depth recording**	
By hand until initial depth		Via camera and ST marks	
Time [min]	**Tip depth [m]**	**penetration rate [mm/min]**	
0.00	0.40	35.29	
2.83	0.50	34.08	
9.68	0.73	27.88	
20.05	0.98	20.08	
35.58	1.25	16.41	
54.17	1.54	13.41	
79.57	1.84	12.01	
106.62	2.17	12.10	
112.63	2.24	11.63	

Table 10: PFE-1 DPT1 data set

Model	Test ID	Date	Soil
PFE-1	DPT2	20150909	WF34
Insertion method		**Depth recording**	
By hand until initial depth		Via camera and ST marks	
Time [min]	**Tip depth [m]**	**penetration rate [mm/min]**	
0.00	0.40	75.02	
1.33	0.50	66.31	
3.02	0.60	59.70	
4.68	0.70	57.69	
6.48	0.80	52.18	
8.52	0.90	45.63	
10.87	1.00	44.28	
13.03	1.10	46.15	
15.20	1.20	42.71	
17.72	1.30	41.24	
20.05	1.40	41.37	
22.55	1.50	41.24	
24.90	1.60	38.59	
27.73	1.70	35.30	
30.57	1.80	36.25	
33.25	1.90	34.19	
36.42	2.00	31.50	
39.60	2.10	32.34	
42.60	2.20	33.24	
45.62	2.30	32.35	
48.78	2.40	29.20	
52.47	2.50	28.50	
55.80	2.60	28.57	
59.47	2.70	27.21	
63.15	2.80	25.42	
67.33	2.90	22.60	
72.00	3.00	19.97	
77.35	3.10	15.35	
85.03	3.20	12.61	
93.22	3.30	10.59	
103.92	3.40	7.17	
121.12	3.50	4.75	
146.02	3.60	3.20	
183.63	3.70	2.32	
232.05	3.80	1.99	
284.17	3.90	1.84	
340.48	4.00	1.62	
407.32	4.10	1.44	
479.20	4.20	1.16	
579.15	4.30	0.94	
692.77	4.40	0.84	
817.22	4.50	0.75	
960.05	4.60	0.64	
1129.67	4.70	0.51	
1353.57	4.80	0.42	
1491.05	4.85	0.36	

Table 11: PFE-1 DPT2 data set

Model	Test ID	Date	Soil
PFE-1	DPT3	20150929	WF34
Insertion method		**Depth recording**	
By hand until initial depth		Via camera and ST marks	
Time [min]	**Tip depth [m]**	**penetration rate [mm/min]**	
0.00	0.40	54.05	
1.85	0.50	51.72	
3.87	0.60	49.79	
5.87	0.70	42.71	
8.55	0.80	35.19	
11.55	0.90	30.69	
15.07	1.00	26.55	
19.08	1.10	22.99	
23.77	1.20	20.31	
28.93	1.30	17.34	
35.30	1.40	14.58	
42.65	1.50	13.45	
50.17	1.60	11.41	
60.18	1.70	10.06	
70.05	1.80	9.88	
80.42	1.90	10.50	
89.10	2.00	11.86	
97.28	2.10	11.73	
106.15	2.20	9.80	
117.68	2.30	8.73	
129.05	2.40	9.07	
139.73	2.50	9.43	
150.27	2.60	9.06	
161.80	2.70	8.94	
172.65	2.80	9.81	
182.18	2.90	10.97	
190.88	3.00	10.41	
201.40	3.10	6.80	
220.28	3.20	3.73	
255.05	3.30	2.28	
308.18	3.40	1.57	
382.55	3.50	1.32	
459.77	3.60	1.20	
549.02	3.70	1.12	
576.08	3.73	1.11	

Table 12: PFE-1 DPT3 data set

Model	Test ID	Date	Soil
PFE-1	DPT4	20151201	WF34
Insertion method		**Depth recording**	
By hand until initial depth		Via camera and ST marks	
Time [min]	**Tip depth [m]**	**penetration rate [mm/min]**	
0.00	0.40	59.42	
1.68	0.50	59.12	
3.38	0.60	56.59	
5.22	0.70	51.95	
7.23	0.80	45.81	
9.58	0.90	39.73	
12.27	1.00	36.04	
15.13	1.10	32.18	
18.48	1.20	27.21	
22.48	1.30	24.44	
26.67	1.40	23.44	
31.02	1.50	23.44	
35.20	1.60	23.44	
39.55	1.70	20.30	
45.05	1.80	14.78	
53.08	1.90	13.00	
60.43	2.00	15.34	
66.12	2.10	18.43	
71.28	2.20	20.65	
75.80	2.30	21.74	
80.48	2.40	19.64	
85.98	2.50	15.77	
93.17	2.60	12.21	
102.37	2.70	9.50	
114.22	2.80	6.54	
132.93	2.90	4.13	
162.67	3.00	2.41	
215.95	3.10	1.58	
289.25	3.20	1.12	
394.20	3.30	0.83	
531.52	3.40	0.67	
685.72	3.50	0.62	

Table 13: PFE-1 DPT4 data set

Model	Test ID	Date	Soil
PFE-2	DPT1	20150130	WF34
Insertion method		**Depth recording**	
By hand until initial depth		Via camera and ST marks	
Time [min]	**Tip depth [m]**	**penetration rate [mm/min]**	
0.00	0.40	39.73	
2.52	0.50	33.24	
6.02	0.60	29.20	
9.37	0.70	28.51	
13.03	0.80	25.48	
17.22	0.90	21.74	
22.23	1.00	19.93	
27.25	1.10	17.78	
32.92	1.19	14.62	
40.93	1.30	13.97	
47.95	1.40	13.30	
55.97	1.50	11.96	
64.67	1.60	10.98	
74.18	1.70	10.32	
84.05	1.80	10.77	
92.75	1.90	8.93	
106.45	2.00	7.53	
119.32	2.10	7.87	
131.85	2.20	8.20	
143.72	2.30	8.25	
156.08	2.40	7.87	
169.12	2.50	7.87	
181.48	2.60	8.09	
193.85	2.70	7.34	
208.72	2.80	4.30	
240.32	2.90	1.21	
374.68	3.00	0.67	
448.60	3.04	0.54	

Table 14: PFE-2 DPT1 data set

Model	Test ID	Date	Soil
PFE-2	DPT2	20160926	WF34
Insertion method		**Depth recording**	
With Mini S/S		With TLM and STATIL	
Time [min]	**Tip depth [m]**	**penetration rate [mm/min]**	
0.00	0.63	48.91	
2.00	0.70	33.14	
5.50	0.81	32.00	
9.50	0.90	29.71	
13.50	1.00	27.43	
22.50	1.20	26.41	
27.50	1.30	25.00	
32.50	1.40	23.00	
37.00	1.50	22.22	
41.50	1.61	22.22	
45.50	1.71	21.33	
49.00	1.80	20.80	
53.00	1.90	20.80	
57.50	2.00	20.00	
62.50	2.10	20.00	
69.00	2.22	20.80	
74.00	2.30	21.33	
80.50	2.40	23.00	
88.00	2.50	24.00	
97.00	2.60	24.00	
108.00	2.70	25.00	
119.50	2.80	27.00	
133.00	2.90	27.00	
149.50	3.00	26.00	
169.50	3.10	24.00	
194.00	3.20	23.00	
221.50	3.30	22.22	
255.00	3.40	20.00	
293.50	3.50	20.00	
337.00	3.60	20.00	
385.50	3.70	18.91	
440.00	3.80	18.18	
509.50	3.90	16.67	
571.50	3.93	15.53	

Table 15: PFE-2 DPT2 data set

Model	Test ID	Date	Soil
PFE-3	DPT1	20160217	WF34
Insertion method		**Depth recording**	
With Mini S/S		With TLM and STATIL	
Time [min]	**Tip depth [m]**	**penetration rate [mm/min]**	
0.00	0.72	35.30	
0.57	0.74	34.33	
2.21	0.80	33.43	
3.92	0.85	32.29	
5.68	0.91	32.29	
7.39	0.96	32.29	
9.15	1.02	32.32	
10.85	1.08	32.39	
12.61	1.13	32.42	
14.30	1.19	33.05	
16.00	1.24	33.10	
17.69	1.30	33.19	
19.37	1.36	32.69	
21.11	1.41	32.73	
22.79	1.47	32.61	
24.55	1.52	32.01	
26.29	1.58	32.69	
27.98	1.64	33.29	
29.66	1.69	33.31	
31.34	1.75	32.71	
33.08	1.80	31.55	
34.89	1.86	31.55	
36.63	1.92	32.10	
38.38	1.97	30.48	
40.31	2.03	29.98	
42.11	2.08	30.46	
43.98	2.14	30.47	
45.79	2.20	30.51	
47.65	2.25	29.54	
49.58	2.31	29.56	
51.44	2.36	29.62	
53.36	2.42	28.26	
55.41	2.48	27.37	
57.45	2.53	26.91	
59.57	2.59	25.43	
61.86	2.64	24.44	
64.15	2.70	23.20	
66.69	2.76	21.57	
69.34	2.81	20.61	
72.12	2.87	19.33	
75.14	2.92	17.83	
78.40	2.98	16.69	
81.85	3.04	15.54	
85.61	3.09	14.41	
89.62	3.15	12.89	
94.30	3.20	11.17	
99.65	3.26	10.09	
105.40	3.32	9.49	
111.46	3.37	8.92	
117.95	3.43	8.27	
125.01	3.48	7.53	
132.82	3.54	6.58	
142.03	3.60	5.94	
151.66	3.65	5.52	
162.31	3.71	4.96	
174.24	3.76	4.37	
187.93	3.82	3.85	
203.34	3.88	3.38	
221.04	3.93	2.98	
240.87	3.99	2.68	
262.89	4.04	2.45	
286.63	4.10	2.35	
310.58	4.16	2.22	
337.14	4.21	1.98	
367.07	4.27	1.57	
405.75	4.32	1.34	

Table 16: PFE-3 DPT1 data set

Model	Test ID	Date	Soil
QM	DPT1	20170927	WF34
Insertion method		**Depth recording**	
With Mini S/S		With TLM and STATIL	
Time [min]	**Tip depth [m]**	**penetration rate [mm/min]**	
0.00	0.65	43.08	
1.40	0.71	41.63	
3.97	0.80	39.34	
7.47	0.90	38.40	
12.40	1.00	35.29	
17.30	1.10	28.74	
22.67	1.20	25.00	
28.27	1.30	22.86	
34.33	1.40	21.43	
40.17	1.50	21.15	
45.53	1.60	21.05	
50.67	1.70	20.34	
55.80	1.80	19.12	
60.93	1.90	18.82	
66.80	2.00	18.82	
72.73	2.10	18.32	
78.82	2.20	17.58	
85.05	2.30	16.84	
91.83	2.40	16.11	
98.60	2.50	15.74	
105.30	2.60	16.55	
111.95	2.70	17.71	
118.73	2.80	18.46	
126.40	2.90	18.90	
135.03	3.00	19.20	
144.60	3.10	19.83	
154.40	3.20	20.08	
165.13	3.30	20.08	
177.50	3.40	19.75	
191.27	3.50	19.43	
208.07	3.60	19.51	
227.67	3.70	18.97	
252.40	3.80	18.46	
286.00	3.90	17.39	
330.33	4.00	16.38	
389.17	4.10	16.16	

Table 17: QM DPT1 data set